

Supporting Information

Forming a metal-free oxidatively-coupled agent, Bicarbazole, as a defect passivation for HTM and an interfacial layer in a p-i-n perovskite solar cell exhibits nearly 20% efficiency

Sudhakar Maddala,¹ Chung-Lin Chung,^{1,2} Shin-Yu Wang,^{1,3} Kalidass Kollimalayan,¹ Hsiang-Lin Hsu,³ Parthasarathy Venkatakrishnan,^{1,4*} Chih-Ping Chen,^{2,*} Yuan Jay Chang^{3,*}

¹*Department of Chemistry, Indian Institute of Technology Madras, Chennai - 600 036, India*

²*Department of Material Engineering, Ming Chi University of Technology, New Taipei City 243, Taiwan*

³*Department of Chemistry, Tunghai University, No.1727, Sec.4, Taiwan Boulevard, Xitun District, Taichung 40704, Taiwan*

⁴*DST-Solar Energy Harnessing Centre (DSEHC), Indian Institute of Technology Madras, Chennai - 600 036, India*

[†]*Equal contribution first author*

Contents

1. Experimental Section	S2-12
2. ¹ H and ¹³ C NMR spectra	S13-20
3. Cost of BC-HTMs	S21-22
4. Oxidative voltammograms and energy level	S23-26
5. Thermal properties (DSC)	S27-28
6. Theoretical calculation	S28-29
7. UV, TRPL and PL spectra of PSCs device	S29
8. Contact angle and surface energy	S30
9. XRD spectra	S31
10. PSC device stability	S32-34
11. Reference	S34-36

*Corresponding author.

E-mail addresses: pvenkat@iitm.ac.in ([P. Venkatakrishnan](mailto:pvenkat@iitm.ac.in)); cpchen@mail.mcut.edu.tw ([C.-P. Chen](mailto:cpchen@mail.mcut.edu.tw)); jaychang@thu.edu.tw ([Y. J. Chang](mailto:jaychang@thu.edu.tw))

1. Experimental Section

General Aspects. All the reagents were used as received from the commercial sources, unless otherwise stated. Dichloromethane (DCM), chloroform, dimethyl sulfoxide (DMSO), *ortho*-dichlorobenzene (*o*-DCB) was dried and distilled over the dehydrating agent CaH₂. Toluene is dried and distilled over sodium-ketyl radical system. Methanol was distilled over magnesium by forming the magnesium cake. To perform the reaction, oven-dried glassware were used under nitrogen gas atmosphere. The progress of the reaction was monitored by TLC (Thin Layer Chromatography) analysis using Merck silica-gel (60 F₂₅₄) precoated plates (0.25 mm). The compounds were visualized to naked-eye under a UV lamp (366 or 254 nm) in a UV chamber or using phosphomolybdic acid (PMA) solution as a stain to detect the compound as a spot. The crude product thus obtained after the reaction was purified by silica-gel (100-200 mesh) column chromatography. A combination of ethyl acetate and hexane was used as the mobile phase. Melting points of the compounds were measured by packing the compound in an open capillary on a melting-point apparatus, and the values were corrected. To record the infrared spectra of the compounds, JASCO FT/IR-4100 spectrometer instrument was used by preparing a dry KBr pellet, and IR signals are quoted in wavenumbers (cm⁻¹). ¹H (400 MHz) and ¹³C (100 MHz) NMR spectra were recorded in ambient temperature using a Bruker Avance FT-NMR (400 MHz) spectrometer in deuterated chloroform (CDCl₃) with TMS as the internal reference. All the chemical shift values were reported in parts per million (ppm, δ). All the reported ¹H NMR spectra were calibrated with the residual proton solvent peak (CDCl₃, δ = 7.26 ppm) or tetramethylsilane (δ = 0.00 ppm), and the ¹³C NMR spectra were referenced to CDCl₃, δ = 77.16 ppm, respectively. The ¹H NMR multiplicities are abbreviated as follows: s, singlet; d, doublet; t, triplet; m, multiplet; dd, doublet of doublet; dt, doublet of triplet and the coupling constants (*J*) values were reported in Hertz (Hz). High-resolution mass spectra (HRMS) were recorded on a Q-TOF Micro micromass spectrometer. UV-visible absorption spectra of compounds in solution were recorded on a AGILENT 8453 diode-array spectrophotometer, and the films were recorded on a JASCO V-650 spectrophotometer. Solvents used for this purpose were of spectroscopic grade, and were purchased commercially.

The starting materials, such as, 9*H*-carbazole, 1,4-dibromobenzene, bromobenzene, copper(I) iodide, L-proline, potassium carbonate, phenylboronic acid, Pd(PPh₃)₄, NBS (*N*-

bromosuccinimide), DDQ (2,3-dichloro-1,4-benzoquinone), MSA (methanesulfonic acid) were purchased commercially and used without further purification, unless otherwise stated. All three monomer derivatives were synthesized according to literature reported procedures (see below)³⁻¹⁰ and were characterized by ¹H, ¹³C NMR, IR spectroscopy techniques as described below, and the data were matched with the literature citations.

UV-visible absorption spectroscopy studies (solution and film)

Optical absorption measurements of compounds in solution were recorded by direct dissolution of the compounds in the dichloromethane solution (4 mg/mL). The thin films were prepared using the spin-coating machine Apex Spin NXG-P1A. The compounds were dissolved in dichloromethane and spin-coated (2500 rpm, 1 min) on a thin quartz glass plate. The films were air-dried. The solution state UV-visible absorption spectra were recorded by using the quartz cuvettes of 1 cm path length and on the solutions of concentration ca. 1.0×10^{-5} M.

Electrochemical studies

Electrochemical experiments were done in a single compartment glass cell at room temperature (25 ± 1 °C). Voltammograms are reported with the positive potential pointing as the positive X-coordinates, and with increasing anodic currents pointing as the positive Y-coordinates. The voltammetric measurements were conducted using the electrochemical workstation (CH Instruments 660A) with the conventional three electrode system. It consists of glassy carbon (area = 0.07 cm^2) as working electrode, which was polished with $0.05 \text{ }\mu\text{m}$ alumina on Buehler felt pads and were ultrasonicated for 1 minute to remove the alumina residue. Platinum wire is used as the counter electrode. All the potentials were taken with the use of a Ag/AgCl, KCl (saturated) reference electrode. All the experiments were conducted in dichloromethane by using the tetrabutylammonium hexafluorophosphate (TBAPF₆, 0.1 M) as the non-aqueous supporting electrolyte under nitrogen gas atmosphere. The concentration of the bicarbazole derivatives was typically ca. 1 mM and the scan rate was 50-100 mV/sec. All the cyclic voltammograms were calibrated using ferrocene as the standard for each experiment and were corrected appropriately.

From the onset of the first oxidation potential, the HOMO values were calculated by using the following equation. The HOMO energy level for the ferrocene/ferrocenium (Fc/Fc⁺) standard is 4.8 eV with respect to the zero vacuum level.

$$E_{\text{HOMO}} \text{ (eV)} = -(E_{\text{OX}}^{\text{onset}} - E_{\text{Fc/Fc}^+}^{\text{onset}}) - 4.80 \text{ eV} \quad \dots \text{ref (1)}$$

LUMO values were derived by adding the HOMO (E_{HOMO}) values with the energy gap (E_{g}), which in turn was obtained from the onset of the UV-visible absorption spectrum.

$$E_{\text{LUMO}} = E_{\text{HOMO}} + E_{\text{g}} \quad \dots \text{ref (2)}$$

Thermal analyses

Thermogravimetric analyses (TGA) were performed on a TGA Q500 V20.10 Build 36 instrument under nitrogen gas atmosphere at a heating rate of 20 °C/min. Differential Scanning Calorimetry (DSC) studies were performed on a DSC Q200 MDSC instrument under nitrogen gas atmosphere at a heating rate of 10 °C/min.

Device Fabrication and Measurements

The ITO-coated glass substrates (sheet resistance: 15 Ω sq⁻¹) were cleaned ultrasonically with abstergent aqueous solution, deionized water, acetone, and isopropyl alcohol for 20 min, and then dried under a stream of N₂. The substrates were then cleaned with air plasma for 10 min. The PEDOT:PSS (CLEVIOS™ P VP AI4083) film was deposited from solution using a spin-rate of 4000 rpm (30 s) and an annealing temperature of 120 °C (20 min). The HTM layers were prepared from a chlorobenzene (CB) solution (10 mg/mL) and deposited on top of ITO using a spin-rate of 3000 rpm. The optimized thickness of the HTM was 10–15 nm. A NiO_x film (ca. 20 nm) was prepared by spin-coating a solution containing the NiO_x precursor [nickel(II) acetylacetonate (129 mg) dissolved in EtOH (5 mL) containing HCl (38 wt%, 50 μL)]. The NiO_x-coated substrates were then baked at 320 °C for 45 min in air. For the bilayer HTL, the HTMs were further spin-coated

(8000 rpm, from a 3 mg/mL solution in CB) on top of NiO_x. The MAPbI₃ precursor solution was prepared by dissolving 1.2 M PbI₂ and MAI (molar ratio, 1:1) in anhydrous DMF/DMSO (4:1). The solution was stirred at 60 °C for 2 h in an Ar-filled glove box. The perovskite precursor solutions were then spin-coated on the HTL-coated substrates with a two-step spin rate (step 1: 2000 rpm for 10 s; step 2: 4000 rpm for 20 s), and then toluene (100 μL) was applied rapidly to the substrates to induce fast crystallization. Finally, the sample was annealed at 100 °C for 10 min to complete the transformation to the perovskite. PC₆₁BM (20 mg mL⁻¹ in anhydrous CB) was deposited; following the deposition of BCP (2 mg mL⁻¹ in IPA), spin-coating was performed at 6000 rpm for 30 s. Finally, the device was completed through the evaporation of Ag or Au contact electrodes (100 nm) at a vacuum level of 10⁻⁷ Pa through a shadow mask. The active area of this electrode was fixed at 0.01 cm².

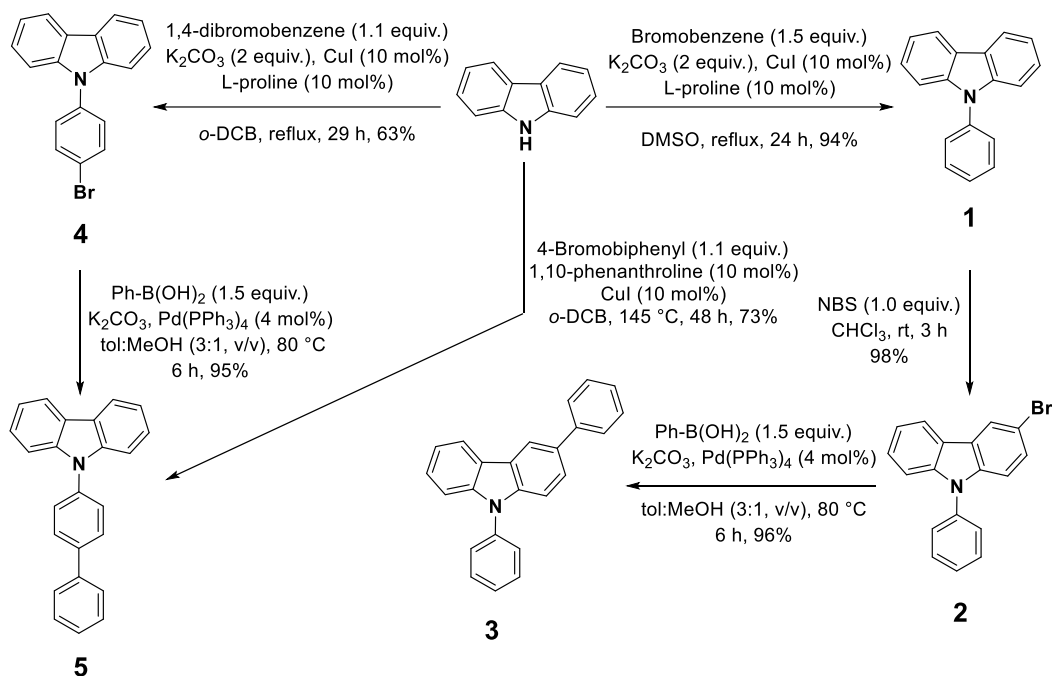
The device performance was measured inside a glove box. The current–voltage (*J–V*) properties of the devices were measured using a computer-controlled Keithley 2400 source measurement unit (SMU) and a Enlitech simulator (AAA Class Solar Simulators) under AM 1.5 illumination (1000 W m⁻²). The illumination intensity was calibrated using a standard Si reference cell and a KG-5 filter. EQEs were measured using an Enlitech QE-R spectral response measurement system to calibrate the current densities of the devices. The morphologies of the perovskites were analyzed through FE-SEM (JEOL JSM 6701F). Grazing-incidence wide-angle X-ray spectroscopy (GIWAXS) was performed using a Philips Panalytical-x’ PertPROMRD instrument; the incident beam angle was above the critical angle (ca. 0.5°). TRPL spectra were recorded using a time-correlated single-photon counting spectrometer (WELLS-001 FX, DongWoo Optron). The pulse laser had a wavelength of 440 nm and an average power of 1 mW; it was operated with a duration of excitation of 2 μs. The SCLC method was used to measure the

hole mobility of the HTMs under the optimized conditions. Hole- and electron-only devices were fabricated having the device structure ITO/PEDOT:PSS/HTM/MoO₃/Ag. The applied voltage (V_{appl}) was corrected from the built-in voltage (V_{bi}); it was the difference in the work function between the bottom electrode (PEDOT:PSS) and the uppermost electrode (MoO₃). When sufficient voltage was applied to these devices, the transport of holes through the HTM layer was limited by the accumulated space-charge. The equation of the SCLC is described by

$$J = \frac{9}{8} \epsilon_r \epsilon_0 \mu_{h,e} \frac{V^2}{L^3}$$

where ϵ_r is the dielectric constant of the material, ϵ_0 is the permittivity of free space (8.85×10^{-12} F m⁻¹), μ_h is the hole mobility, V is the device's applied voltage, and L is the HTM thickness (30 nm).

Synthesis: *Experimental procedure*



Scheme S1: Synthesis of the carbazole monomers.

9-Phenyl-9H-carbazole (**1**)³

Into a two-neck 100 mL round-bottom flask, carbazole (3.0 g, 17.9 mmol) was taken and dissolved in dry DMSO (dimethyl sulfoxide, 30 mL) solvent. To this, bromobenzene (4.22 g, 26.9 mmol), K_2CO_3 (5.0 g, 36 mmol), L-proline (0.20 g, 1.8 mmol), CuI (0.34 g, 1.8 mmol) were added. The reaction contents were refluxed for 24 hours, and the course of the reaction was monitored by the thin layer chromatography (TLC). As soon as the starting material was consumed completely, the contents were cooled down to room temperature, and DMSO was distilled off through vacuum-distillation. The crude reaction mixture was extracted with water (80 mL) and ethyl acetate (3 \times 70 mL). The combined organic layer was washed with brine solution, dried over anhydrous Na_2SO_4 , filtered and the solvent was evaporated via rotary evaporator. The crude product thus obtained was purified by silica-gel column chromatography using hexane as the eluent to afford a white color solid as the pure product (4.12 g, 16.93 mmol, 94%).

White color solid. R_f = 0.8 (9:1, hexane/EtOAc). Mp: 88-90 °C (lit.⁴ 89-90 °C); IR (KBr), cm^{-1} : 3060, 2962, 1624, 1597, 1502, 1478, 1452, 1431, 1362, 1336, 1318, 1232, 1179, 1120, 1074, 1026, 1002. 1H NMR (400 MHz, $CDCl_3$): δ 8.15 (d, J = 7.6 Hz, 2H), 7.64-7.55 (m, 4H), 7.47 (t, J = 6.8

Hz, 1H), 7.43-7.38 (m, 4H), 7.32-7.26 (m, 2H). $^{13}\text{C}\{^1\text{H}\}$ NMR)100 MHz, CDCl_3 (: δ 141.1, 137.9, 130.0, 127.6, 127.3, 126.1, 123.5, 120.4, 120.0, 109.9.

*3-Bromo-9-phenyl-9H-carbazole (2)*⁵

To a solution of 9-phenyl-9H-carbazole (1.0 g, 4.12 mmol) in chloroform (30 mL), was added N-bromosuccinimide (0.73 g, 4.12 mmol) in several portions with 10 minutes interval. The reaction contents were stirred at room temperature for 3 hours. The course of the reaction was monitored with thin layer chromatography. After complete consumption of the starting material, the reaction mixture was poured into water, and the organic contents were extracted into chloroform (3 \times 25 mL). The combined organic layer was washed with brine solution, dried over anhydrous Na_2SO_4 , filtered and the solvent was evaporated to dryness via rotary evaporator. The crude product was then purified by silica-gel column chromatography using hexane as the eluent to afford the colorless solid as the pure product (1.29 g, 4.01 mmol, 98%).

Colorless solid. R_f = 0.83 (9:1, hexane/EtOAc). Mp: 76-78 °C (lit.⁴ 79-80 °C). IR)KBr, cm^{-1} (: 3062, 3011, 2918, 1598, 1501, 1469, 1315, 1270, 1231, 1167, 1056, 1025. ^1H NMR)400 MHz, CDCl_3 (: δ 8.25 (d, J = 1.2 Hz, 1H), 8.09 (d, J = 8.0 Hz, 1H), 7.61 (t, J = 7.6 Hz, 2H), 7.53 (d, J = 7.2 Hz, 2H), 7.49 (t, J = 8.4 Hz, 2H), 7.45-7.36 (m, 2H), 7.33-7.26 (m, 2H). $^{13}\text{C}\{^1\text{H}\}$ NMR)100 MHz, CDCl_3 (: δ 141.3, 139.6, 137.3, 130.1, 128.7, 127.8, 127.1, 126.8, 125.2, 123.1, 122.4, 120.6, 120.4, 112.8, 111.3, 110.1.

*3,9-Diphenyl-9H-carbazole (3)*⁶

A 100 mL round-bottom flask was loaded with 3-bromo-9-phenyl-9H-carbazole (2.0 g, 6.21 mmol), phenylboronic acid (1.13 g, 9.3 mmol), potassium carbonate (2.6 g, 18.6 mmol), and mixture of toluene and methanol (3:1, v/v, 40 mL) under nitrogen gas atmosphere. The reaction mixture was degassed over 20 minutes and $\text{Pd}(\text{PPh}_3)_4$ (0.29 g, 0.25 mmol) was introduced. The contents were heated at 85 °C for 12 h. After consumption of the starting material (indicated on TLC), the reaction mixture was cooled to room temperature, it was then added to water (10 mL). The organic portions were extracted into ethyl acetate (3 \times 30 mL). The combined organic layer was washed with brine solution, dried over anhydrous Na_2SO_4 , filtered and the organic solvent was removed to dryness at the rotary evaporator. The crude product was purified by silica-gel

column chromatography using hexane as the eluent to afford the product in excellent yield (1.9 g, 5.95 mmol, 96%).

White color solid. $R_f = 0.78$ (9:1, hexane/EtOAc). Mp: 159-161 °C. IR (KBr, cm^{-1}): 3060, 3033, 1598, 1501, 1474, 1456, 1363, 1329, 1299, 1233, 1050. ^1H NMR (400 MHz, CDCl_3): δ 8.36 (s, 1H), 8.19 (d, $J = 7.6$ Hz, 1H), 7.73 (d, $J = 7.2$ Hz, 2H), 7.69-7.57 (m, 5H), 7.53-7.46 (m, 4H), 7.45-7.41 (m, 2H), 7.35 (t, $J = 8.0$ Hz, 1H), 7.31 (m, 1H). $^{13}\text{C}\{^1\text{H}\}$ NMR (100 MHz, CDCl_3): δ 142.1, 141.5, 140.5, 137.8, 133.6, 130.0, 128.9, 127.6, 127.4, 127.1, 126.7, 126.2, 125.6, 124.0, 123.6, 120.5, 120.2, 118.9, 110.1, 110.0.

9-(4-Bromophenyl)-9H-carbazole (**4**)⁷

Into a two-neck 100 mL round-bottom flask equipped with a magnetic stir-bar, carbazole (3.0 g, 17.9 mmol) was taken and dissolved in *o*-DCB (*ortho*-dichlorobenzene, 30 mL). To this solution, 1,4-dibromobenzene (4.6 g, 19.7 mmol), K_2CO_3 (5.0 g, 36 mmol), L-proline (0.21 g, 1.8 mmol), CuI (0.34 g, 1.8 mmol) were added, and the reaction contents were refluxed for 29 hours. As soon as the starting material was consumed (as noticed on the TLC), the reaction contents were cooled to room temperature and the solvent was distilled out by means of vacuum-distillation. To this crude residue water (50 mL) was introduced. The organics were extracted into ethyl acetate (3 \times 70 mL). The combined organic layer was washed with brine solution, dried over anhydrous Na_2SO_4 , filtered, and the organic solvent was evaporated under reduced pressure. The crude product was purified by silica-gel column chromatography using hexane as the eluent to afford the product (3.64 g, 11.3 mmol, 63%).

White color solid. $R_f = 0.68$ (9:1, hexane/EtOAc). Mp: 142-144 °C (lit.⁸ 143-146 °C). IR (KBr, cm^{-1}): 3052, 2968, 1622, 1591, 1492, 1450, 1360, 1333, 1317, 1229, 1178, 1069, 1007. ^1H NMR (400 MHz, CDCl_3): δ 8.14 (d, $J = 8.0$ Hz, 2H), 7.73 (d, $J = 8.8$ Hz, 2H), 7.45 (d, $J = 8.8$ Hz, 2H), 7.42 (t, $J = 8.0$ Hz, 2H), 7.37 (d, $J = 8.0$ Hz, 2H), 7.30 (t, $J = 8.0$ Hz, 2H). $^{13}\text{C}\{^1\text{H}\}$ NMR (100 MHz, CDCl_3): δ 140.8, 137.0, 133.3, 128.9, 126.2, 123.7, 121.1, 120.5, 120.4, 109.7.

9-(1,1'-Biphenyl-4-yl)-9H-carbazole (**5**)⁹

A 100 mL two-neck round-bottom flask was loaded with 9-(4-bromophenyl)-9H-carbazole (1.3 g, 4.0 mmol), phenylboronic acid (0.69 g, 5.6 mmol), potassium carbonate (1.56 g, 11.3 mmol),

and mixture of toluene and methanol (3:1, v/v, 28 mL) under nitrogen gas atmosphere. The reaction mixture was degassed over 20 minutes and then Pd(PPh₃)₄ (0.19 g, 0.16 mmol) was introduced under nitrogen gas atmosphere. The contents were heated at 80 °C for 12 h and the progress of the reaction was monitored by TLC. After disappearance of the starting material (as noticed by TLC), the reaction contents were cooled to room temperature. The organic contents were extracted with water (20 mL) and ethyl acetate (3 × 30 mL). The combined organic layer was washed with brine solution, dried over anhydrous Na₂SO₄, filtered, and the organic solvent was removed under reduced pressure at the rotary evaporator. The crude product was finally purified by silica-gel column chromatography using hexane as the eluent to afford the product in good yield (1.2 g, 3.84 mmol, 95%).

White color solid. *R_f* = 0.51 (9:1, hexane/EtOAc). Mp: 180-182 °C (lit.¹⁰ 181-184 °C). IR (KBr, cm⁻¹): 3051, 2914, 2855, 1655, 1592, 1518, 1486, 1451, 1330, 1228, 1102, 1074, 1008. ¹H NMR (400 MHz, CDCl₃): δ 8.17 (d, *J* = 8.0 Hz, 2H), 7.83 (d, *J* = 8.0 Hz, 2H), 7.70 (d, *J* = 8.0 Hz, 2H), 7.65 (d, *J* = 8.0 Hz, 2H), 7.52 (t, *J* = 7.6 Hz, 2H), 7.49 (d, *J* = 8.0 Hz, 2H), 7.44 (t, *J* = 7.6 Hz, 2H), 7.42 (t, *J* = 6.8 Hz, 1H), 7.32 (t, *J* = 6.8 Hz, 2H). ¹³C{¹H} NMR (100 MHz, CDCl₃): δ 141.0, 140.48, 140.45, 137.1, 129.1, 128.7, 127.8, 127.5, 127.3, 126.1, 123.6, 120.5, 120.1, 110.0.

Synthesis of 3,3'-Bicarbazoles via the Oxidative C-C coupling method

A general procedure for the synthesis of 3,3'-bicarbazole derivatives from the corresponding carbazole monomers via oxidative coupling is reported below.

General Procedure for the Oxidative Coupling of Carbazoles. The carbazole monomer (0.8 mmol, 1.0 equiv.) dissolved in dry dichloromethane (DCM, 10.0 mL) was cooled to 0 °C, and methanesulfonic acid (MSA) was introduced slowly at this temperature. After stirring the contents at this temperature for 5 minutes, DDQ (2,3-dichloro-5,6-dicyano-1,4-benzoquinone, 0.370 g, 1.6 mmol, 2.0 equiv) was added. The reaction mixture turns to deep blue color immediately. The progress of the reaction was monitored by TLC (thin-layer chromatography) regularly. As soon as the starting material was found disappeared completely, as observed by TLC, the saturated sodium bicarbonate solution was carefully added under ice-cold conditions. The reaction mixture was

transferred into the separating funnel, and the organic contents were extracted into chloroform (3 × 10 mL). The combined organic layer was washed again with saturated sodium bicarbonate solution, followed by brine solution. It is noticeable that the aqueous (saturated sodium bicarbonate) layer appeared deep red color, and the organic portion remained colorless. Finally, the organic layer was dried over anhydrous Na₂SO₄, filtered, and the organic solvent was evaporated at the rotary evaporator. The crude product thus obtained was further purified by silica-gel column chromatography using hexane-ethyl acetate mixtures as the mobile phase. The pure products obtained were white powders.

*9,9'-Diphenyl-9H,9'H-3,3'-bicarbazole (NP-BC)*¹¹

The reaction mixture containing 9-phenyl-9H-carbazole (0.75 g, 3.08 mmol), DDQ (1.4 g, 6.16 mmol), DCM (38 mL), and MSA (3.75 mmol) was stirred at room temperature for one minute and then quenched. It was further purified as mentioned in the general procedure.

Time: 1 min. Yield: 0.71g, 95%. Dull white solid. R_f = 0.35 (19:1, hexane/EtOAc). Mp: 200-202 °C (lit.¹¹ 200 °C). IR (KBr, cm⁻¹): 3050, 2929, 2851, 1596, 1499, 1453, 1359. ¹H NMR (400 MHz, CDCl₃): δ 8.47 (d, *J* = 1.6 Hz, 2H), 8.25 (d, *J* = 7.6 Hz, 2H), 7.79 (dd, *J* = 8.8 and 1.6 Hz, 2H), 7.67-7.61 (m, 8H), 7.52 (d, *J* = 8.4 Hz, 2H), 7.52-7.41 (m, 6H), 7.33 (dt, *J* = 8.0 and 2.4 Hz, 2H). ¹³C{¹H} NMR (100 MHz, CDCl₃): δ 141.5, 140.2, 137.9, 134.5, 130.0, 127.5, 127.2, 126.2, 126.0, 124.1, 123.7, 120.6, 120.1, 119.0, 110.1, 110.0. HRMS (ESI-TOF) *m/z*: [M + H]⁺ calcd for C₃₆H₂₅N₂, 485.2018, found *m/z* = 485.2032.

*6,6',9,9'-Tetraphenyl-9H,9'H-3,3'-bicarbazole (PNP-BC)*¹²

The reaction mixture containing 3,9-diphenyl-9H-carbazole (0.3 g, 0.94 mmol), DDQ (0.43 g, 1.88 mmol), DCM (12 mL), and MSA (1.15 mL) was stirred at room temperature for one minute, and then quenched. The compound isolated was purified as mentioned in the general procedure.

Time: 1 min. Yield: 0.28 g, 95%. Dull-white color crystalline solid. R_f = 0.4 (19:1, hexane/EtOAc). Mp: 117-119 °C. IR (KBr, cm⁻¹): 3048, 1638, 1594, 1499, 1472, 1452, 1410, 1363, 1272, 1233. ¹H NMR (400 MHz, CDCl₃): δ 8.53 (s, 2H), 8.47 (s, 2H), 7.82 (dd, *J* = 8.4 and 1.6 Hz, 2H), 7.79-7.75 (m, 4H), 7.69 (dd, *J* = 8.4 and 1.6 Hz, 2H), 7.67-7.62 (m, 8H), 7.56-7.47 (m, 10H), 7.35 (t, *J* = 6.8 Hz, 2H). ¹³C{¹H} NMR (100 MHz, CDCl₃): δ 142.1, 141.0, 140.6, 137.9, 134.5, 133.7, 130.1,

128.9, 127.7, 127.5, 127.2, 126.7, 126.1, 125.7, 124.30, 124.26, 119.09, 119.04, 110.4, 110.3.
HRMS (ESI-TOF) m/z : $[M + Na]^+$ calcd for $C_{48}H_{32}N_2Na$, 659.2463, found 659.2438.

*9,9'-Di([1,1'-biphenyl]-4-yl)-9H,9'H-3,3'-bicarbazole (NBP-BC)*¹³

The reaction contents 9-(1,1'-biphenyl-4-yl)-9H-carbazole (0.3 g, 0.94 mmol), DDQ (0.43 mg, 1.88 mmol), and DCM (12 mL), MSA (1.15 mL) were stirred at room temperature for one minute and then quenched. Purification of the compound was done by recrystallization from hot chloroform-methanol (1:1, v/v) mixtures. Because the solubility of the compound is relatively less to perform purification using column chromatography.

Time: 1 min (DDQ). Yield: 0.29 g, 96%. White amorphous solid. $R_f = 0.4$)19:1, hexane/EtOAc(.
Mp: 220 °C. IR)KBr, cm^{-1} (: 1658, 1638, 1618, 1563, 1556, 1522, 1485, 1448, 1415. 1H NMR)400 MHz, $CDCl_3$ (: δ 8.48 (s, 2H), 8.26 (d, $J = 7.6$ Hz, 2H), 7.86 (d, $J = 8.4$ Hz, 4H), 7.81 (d, $J = 8.4$ Hz, 2H), 7.76-7.68 (m, 8H), 7.59 (d, $J = 8.4$ Hz, 2H), 7.56-7.49 (m, 6H), 7.49-7.39 (m, 4H), 7.34 (t, $J = 8.0$ Hz, 2H). $^{13}C\{^1H\}$ NMR)100 MHz, $CDCl_3$ (: δ 141.5, 140.5, 140.2, 137.1, 134.6, 129.1, 128.7, 127.8, 127.4, 127.3, 126.3, 126.0, 124.2, 123.8, 120.6, 120.2, 119.1, 110.3, 110.1.
HRMS (ESI-TOF) m/z : $[M]^+$ calcd for $C_{48}H_{32}N_2Na$, 636.2565, found 636.2561.

2. ^1H and ^{13}C NMR spectra

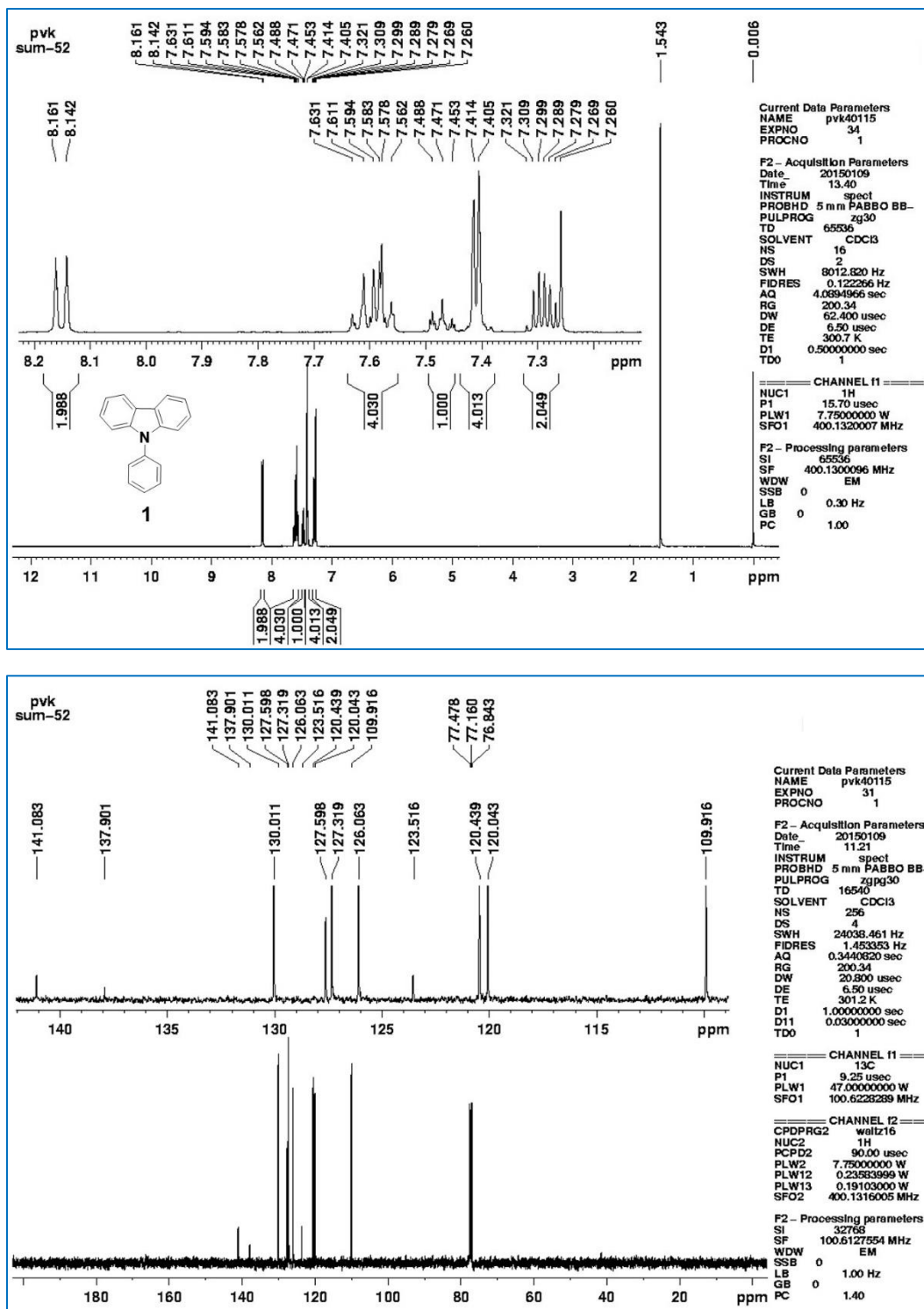


Figure S1. ^1H (top) & ^{13}C NMR (bottom) spectrum of 9-phenyl-9H-carbazole (1) in CDCl_3 .

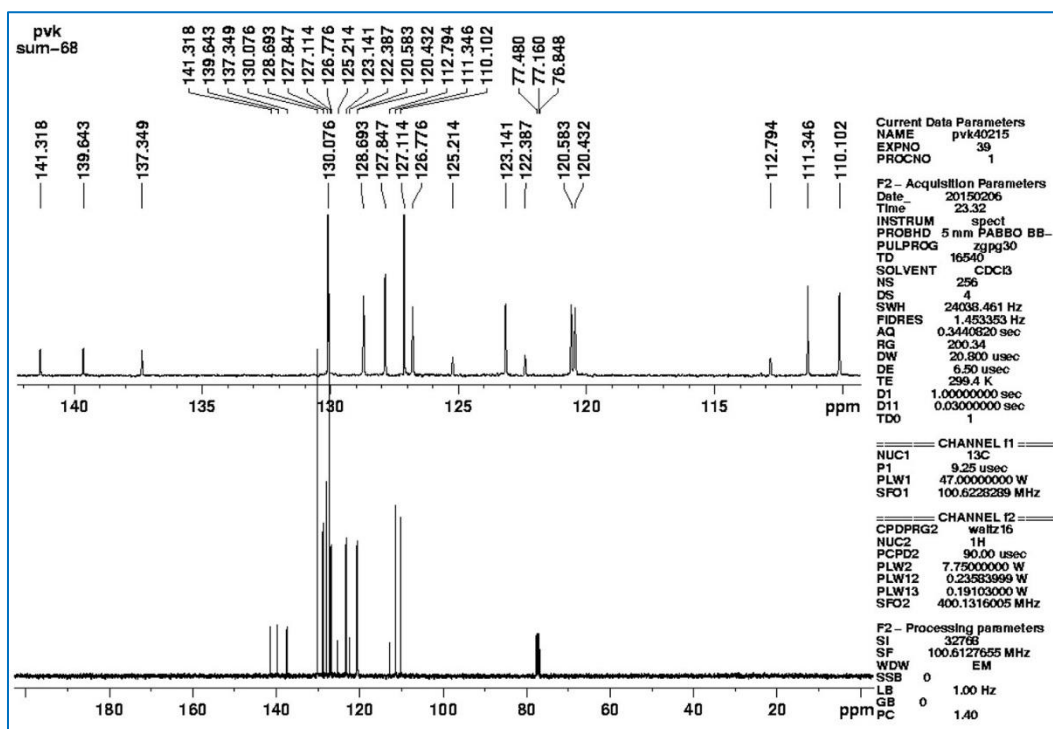
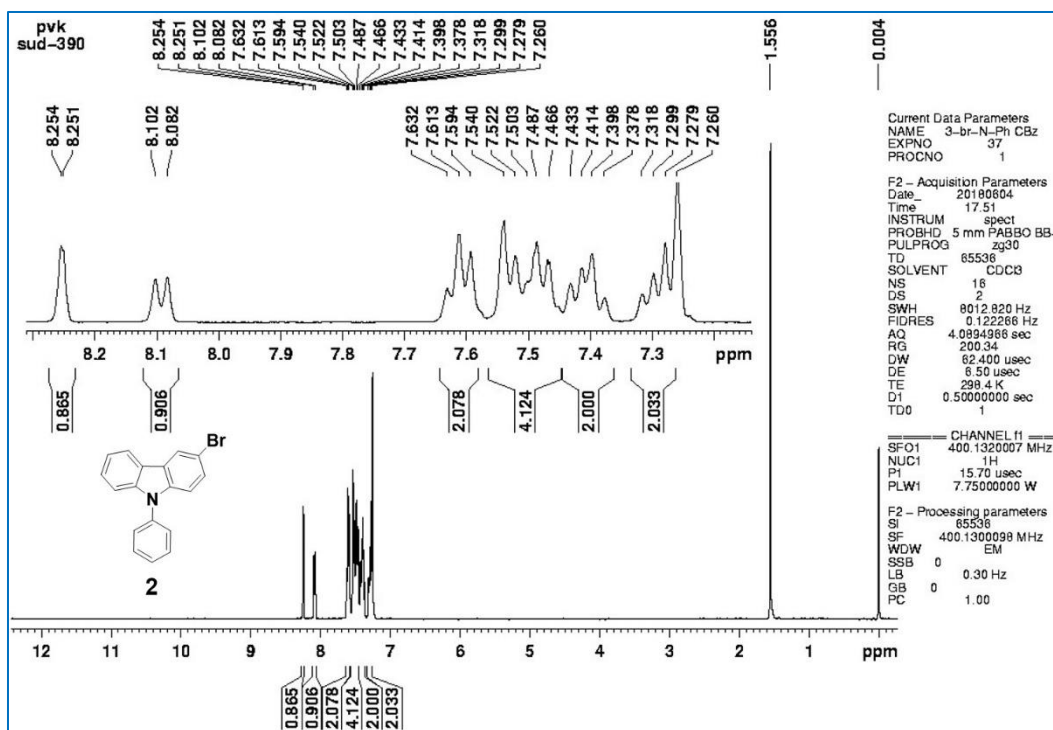


Figure S2. ^1H (top) & ^{13}C NMR (bottom) spectrum of 3-bromo-9-phenyl-9H-carbazole (2) in CDCl_3 .

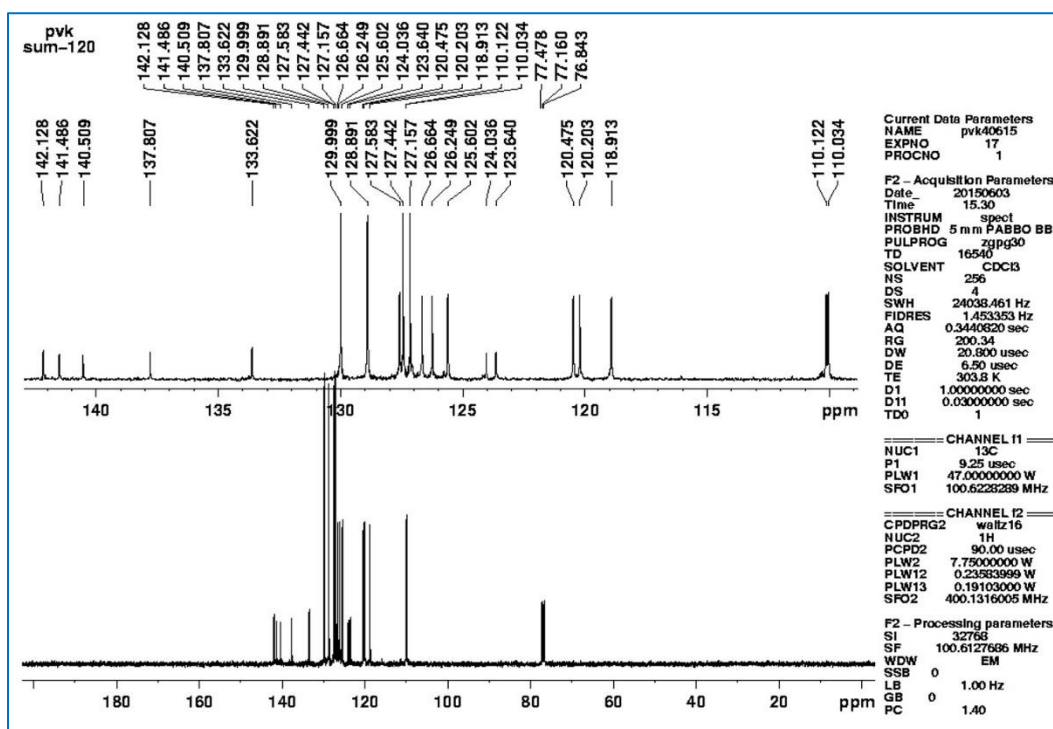
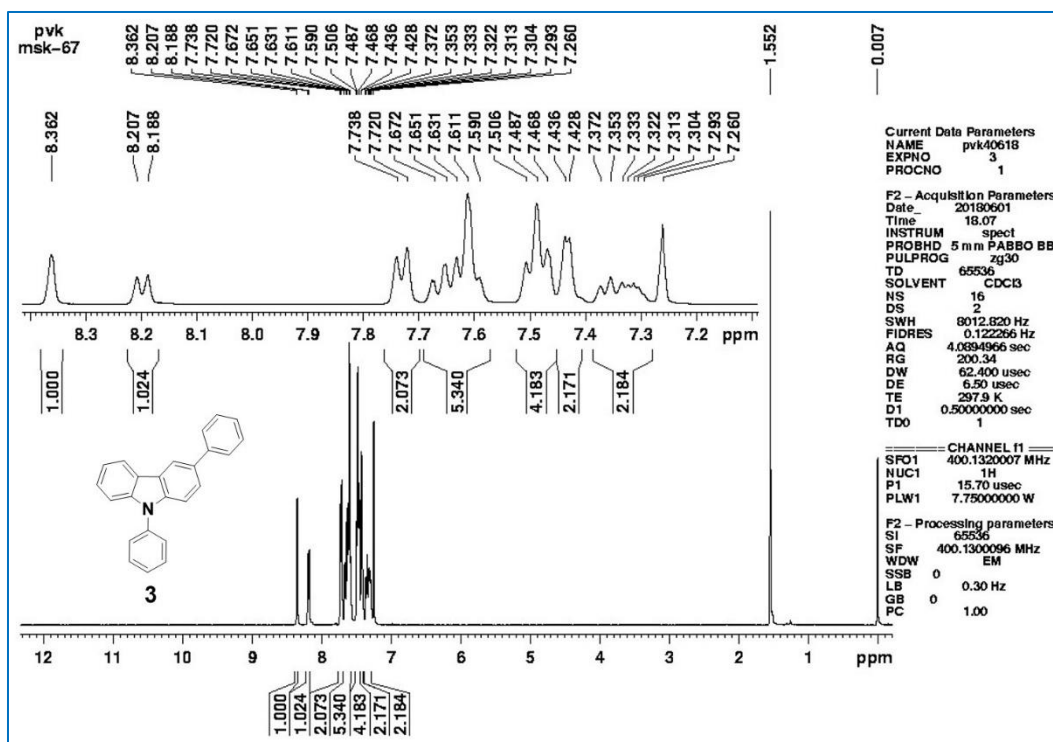


Figure S3. ^1H (top) & ^{13}C NMR (bottom) spectrum of 3,9-diphenyl-9H-carbazole (3) in CDCl_3 .

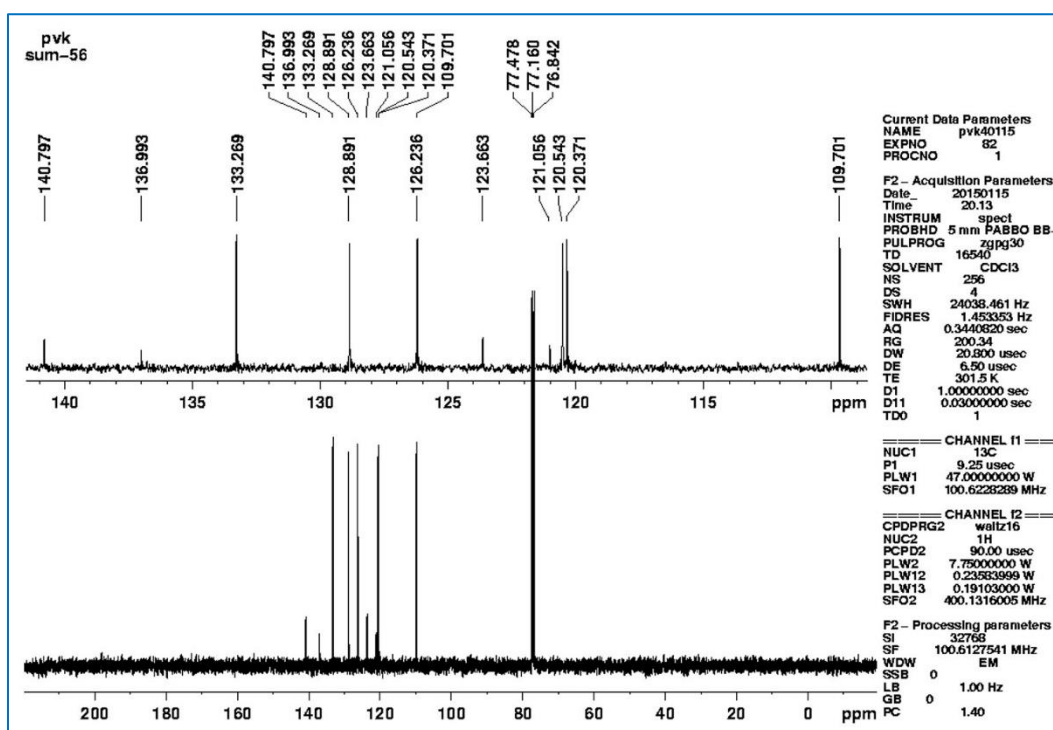
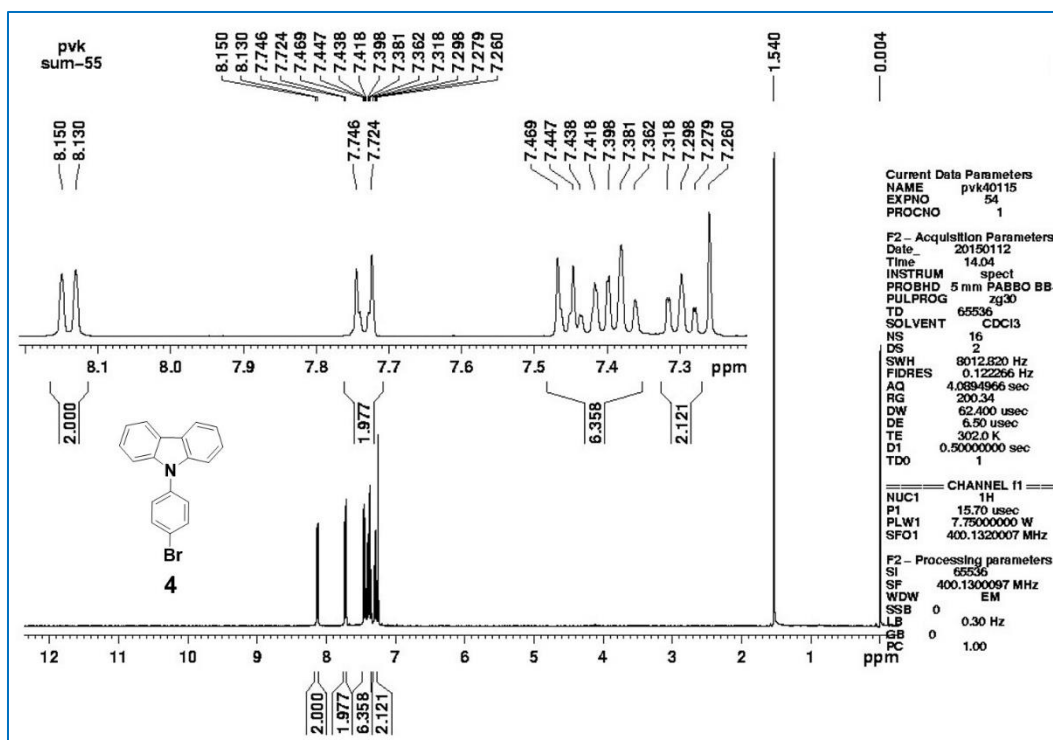


Figure S4. ^1H (top) & ^{13}C NMR (bottom) spectrum of 9-(4-bromophenyl)-9H-carbazole (4) in CDCl_3 .

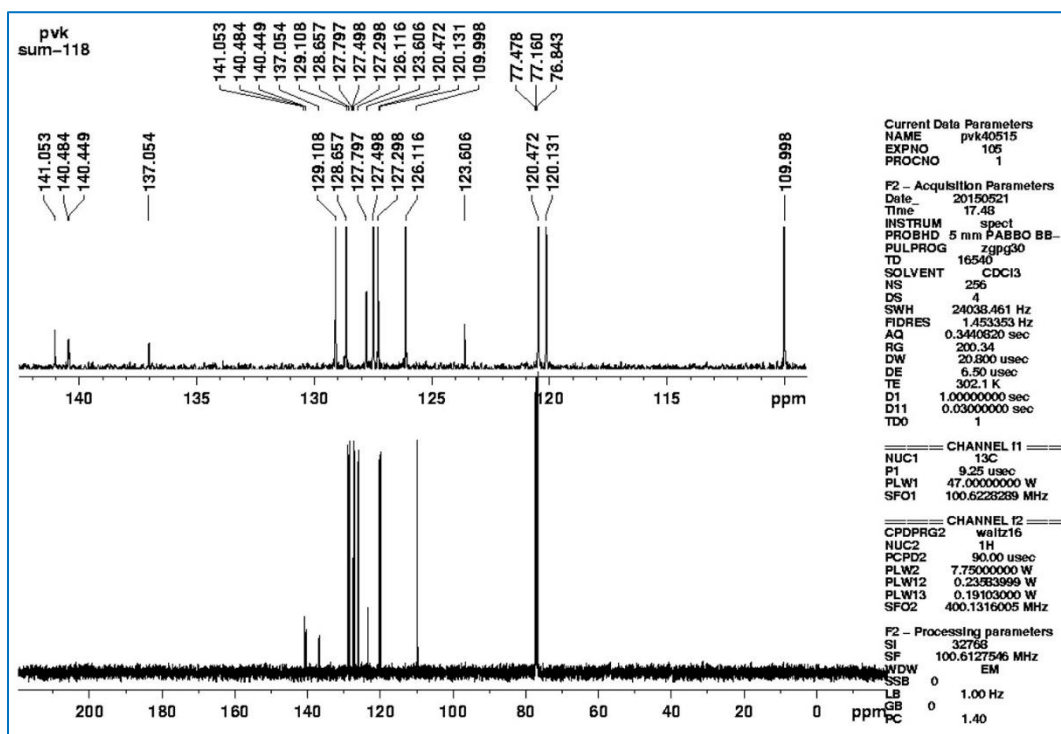
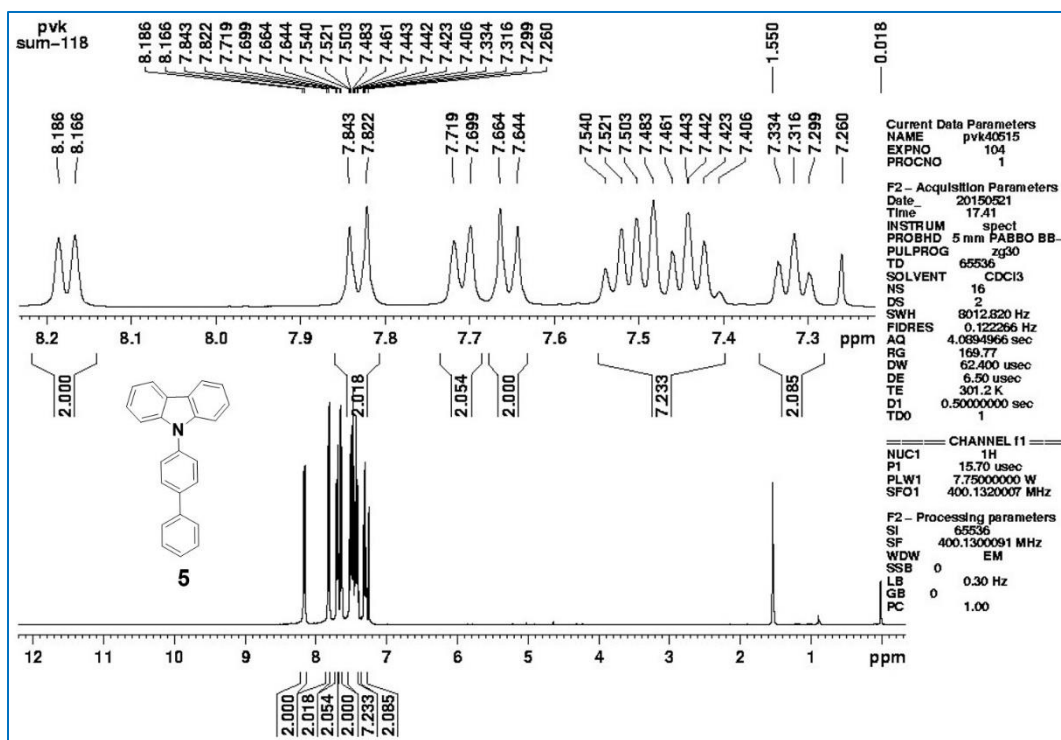


Figure S5. ^1H (top) & ^{13}C NMR (bottom) spectrum of 9-(1,1'-biphenyl-4-yl)-9H-carbazole (5) in CDCl_3 .

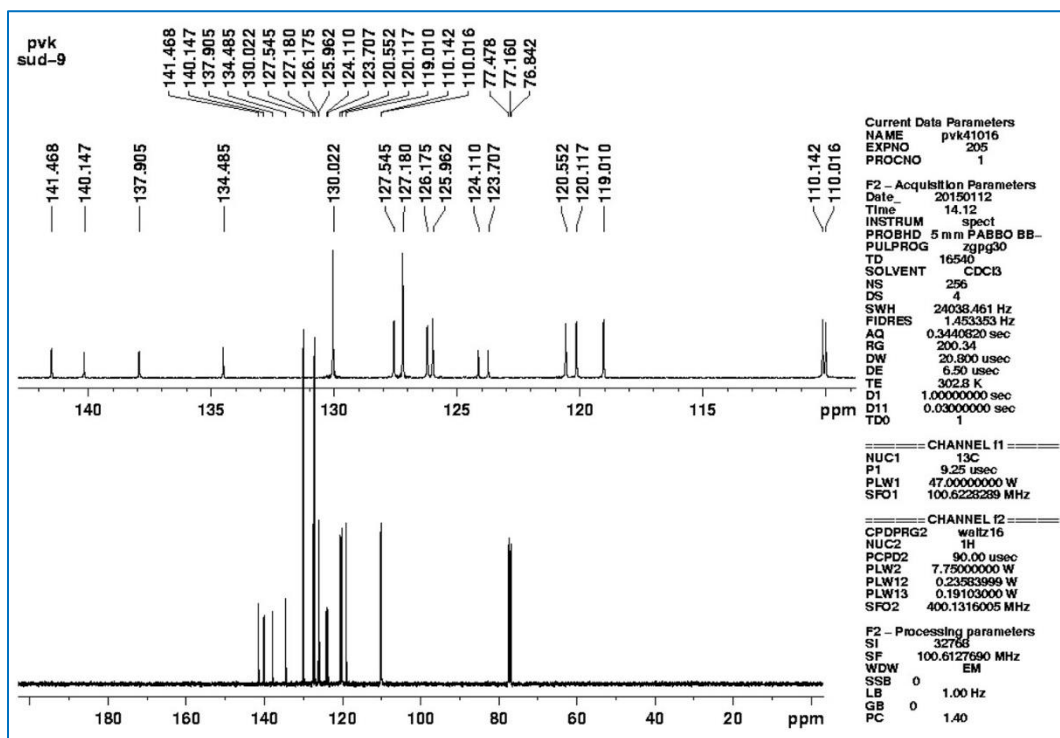
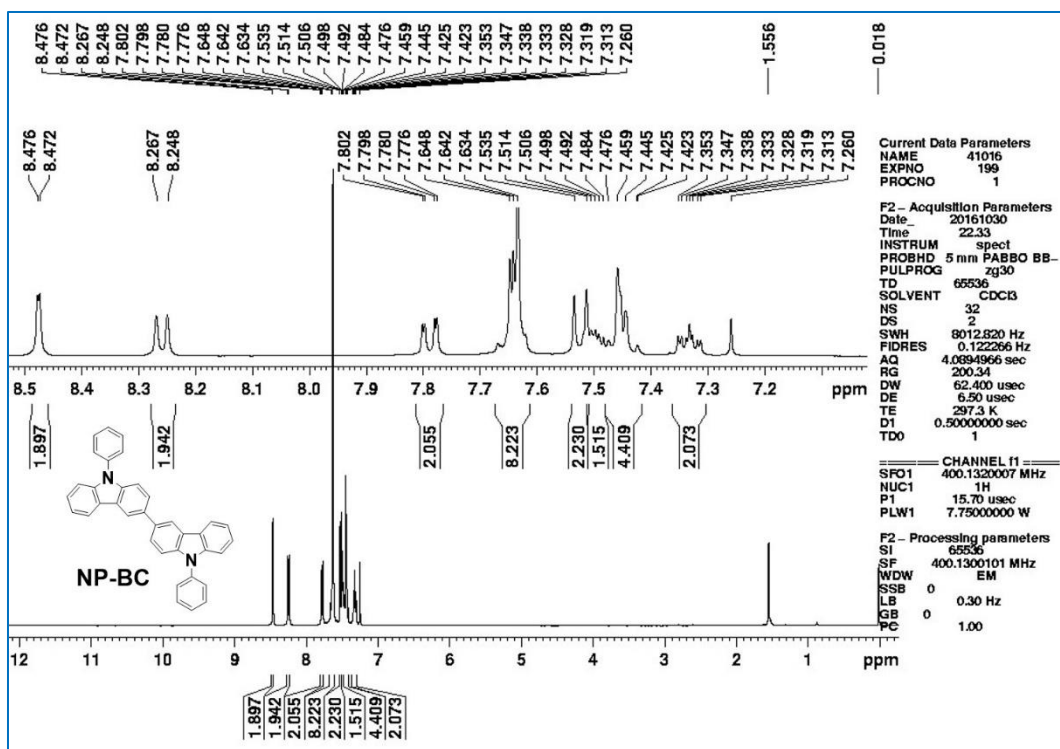


Figure S6. ^1H (top) & ^{13}C NMR (bottom) spectrum of NP-BC in CDCl_3 .

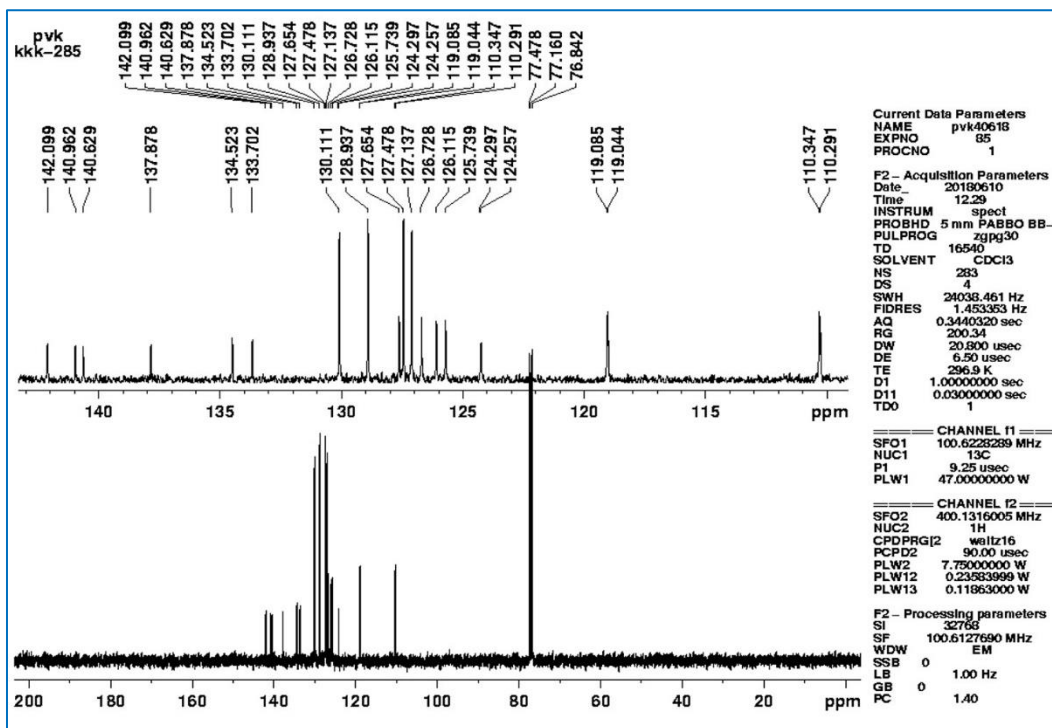
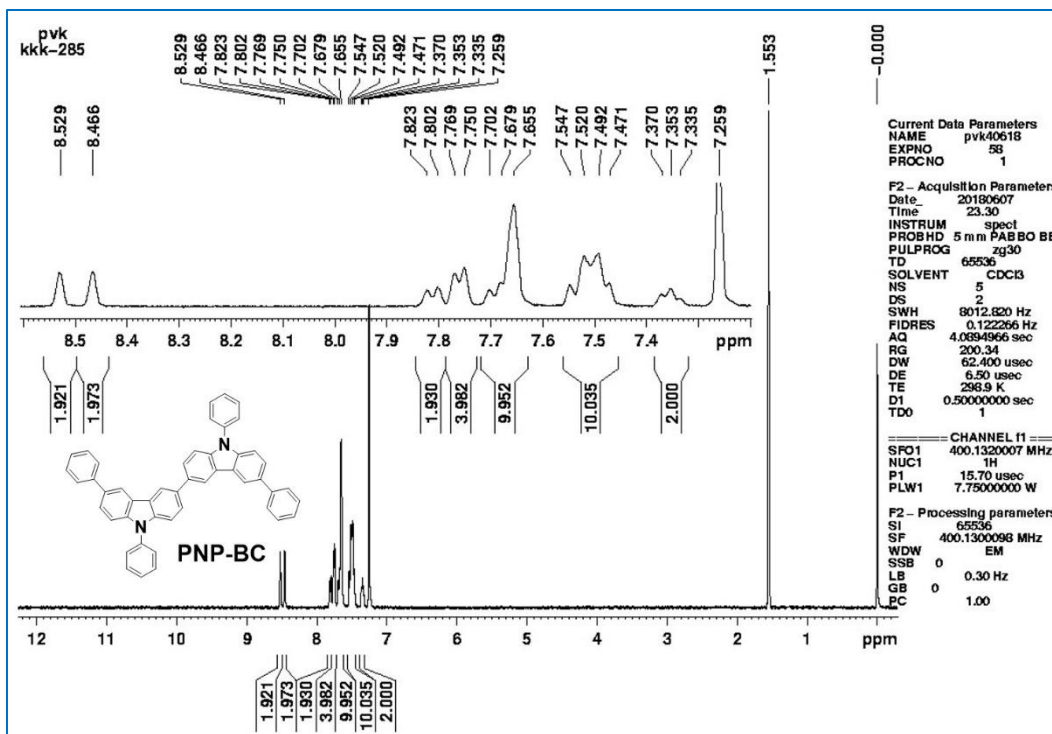


Figure S7. ^1H (top) & ^{13}C NMR (bottom) spectrum of PNP-BC in CDCl_3 .

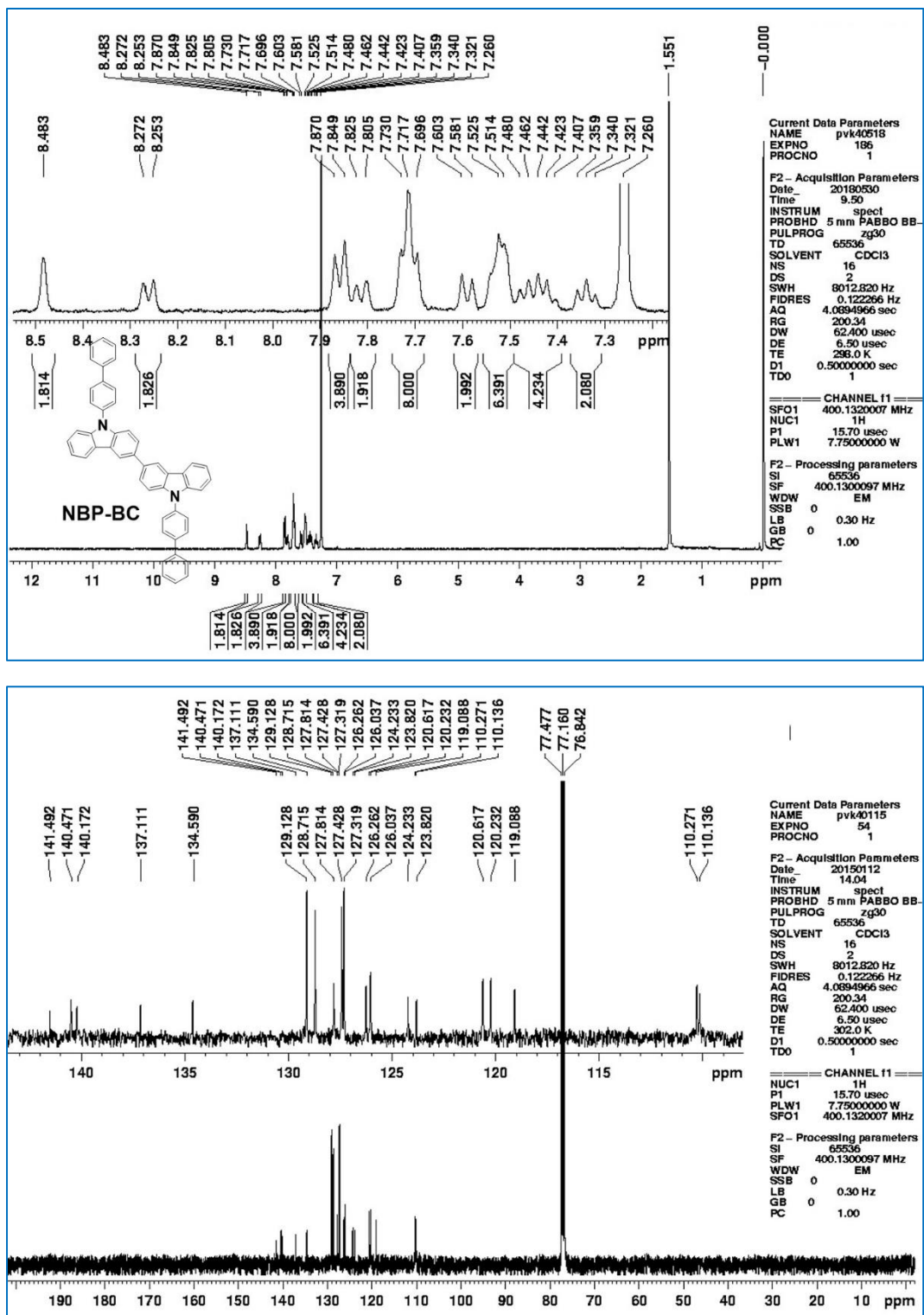
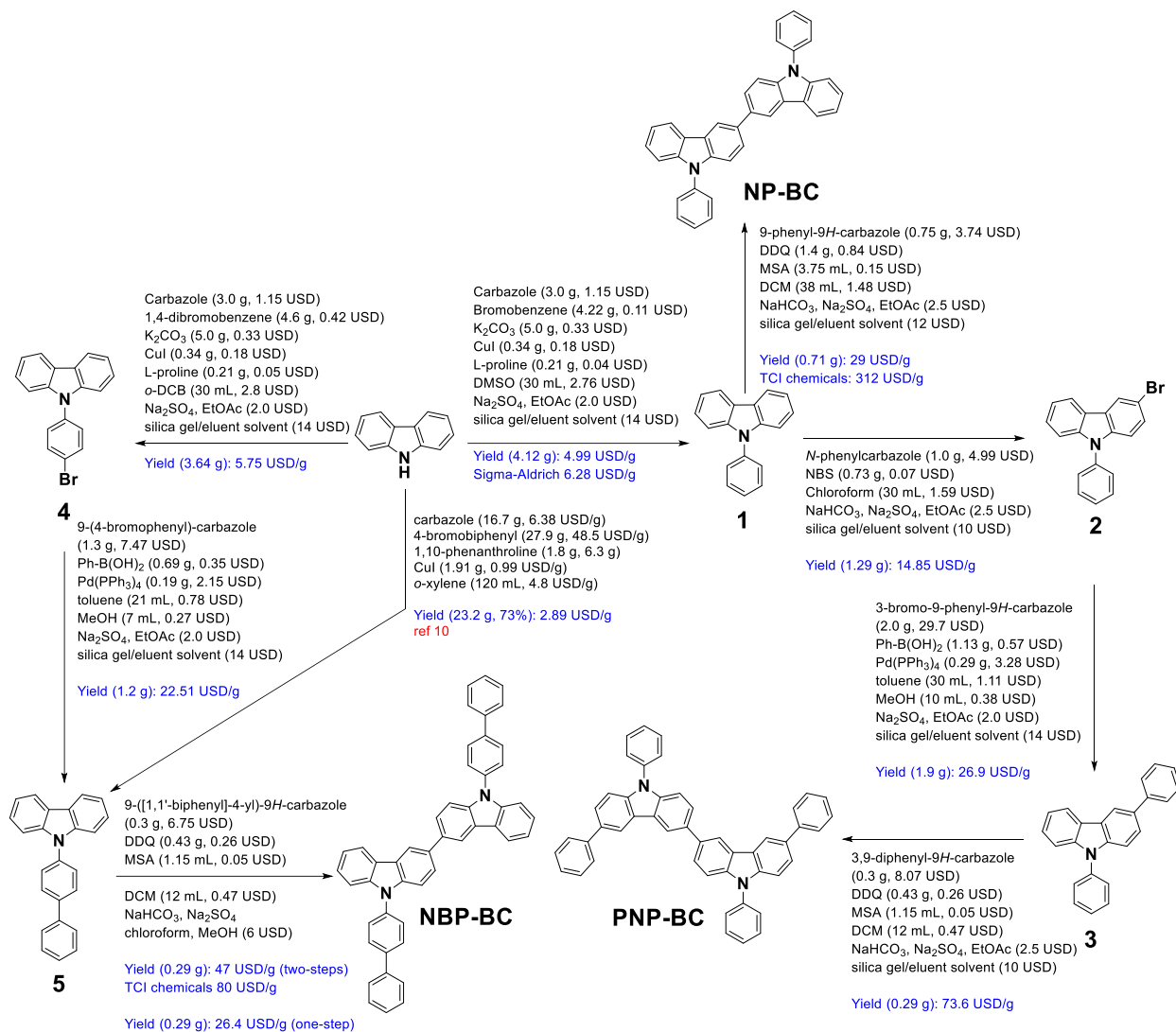


Figure S8. ¹H (top) & ¹³C NMR (bottom) spectrum of NBP-BC in CDCl₃.

3. Cost of BC-HTMs



Scheme S2. Step-wise cost analysis for the synthesis of BC-HTMs.

Table S1. Comparison cost and the performance of various HTMs based PSCs

Dye	PSCs device type	Cost (USD/g)	PSCs efficiency	Ref.
SFX-MeOTAD	n-i-p	16.87	12.40%	14
FDT	n-i-p	34.43	20.2%	15
X60	n-i-p	33.89	19.84%	16
Yih-2	n-i-p	29.14	16.06%	17
TPA-ANT-TPA	n-i-p	~67	17.5%	18
EDOT-Amide-TPA	n-i-p	~5	20.3%	19
NP-BC	p-i-n	33.99	11.84% 19.49%(as interfacial layer)	This work

Table S2. Calculated cost of the BC-HTMs, starting from the simple carbazole.

HTM	Carbazole	Bromo benzene	K ₂ CO ₃	CuI	L-proline	DDQ	MSA	Price
Spiro-OMeTAD								460 USD/ g
PTAA								1980 USD/g
NPB								132 USD/g
PEDOT:PSS								1220 USD/L (1.4 wt%)
Chemical	41 USD /100 g	13 USD /500 g	33 USD /500 g	13 USD / 25 g	5 USD /25 g	60 USD /100 g	10 USD /250 mL	
NP-BC	9-phenyl-9 <i>H</i> -carbazole: 4.99 USD/g; NP-BC: 29 USD/g.							Total: 33.99 USD/g
PNP-BC	9-phenyl-9 <i>H</i> -carbazole: 4.99 USD/g; 3-Bromo-9-phenyl-9 <i>H</i> -carbazole: 14.85 USD/g; 3,9-diphenyl-9 <i>H</i> -carbazole: 26.9 USD/g; PNP-BC: 73.6 USD/g.							Total: 120.34 USD/g
NBP-BC	9-(4-bromophenyl)-9 <i>H</i> -carbazole: 5.75 USD/g; 9-([1,1'-biphenyl]-4-yl)-9 <i>H</i> -carbazole: 22.51 USD/g; NBP-BC: 47 USD/g.							Total: 75.26 USD/g

4. Oxidative voltammograms and energy level

From the onset of the UV-visible spectrum, the energy values were calculated by using the following equation.

$$E_g = 1240/\lambda^{\text{onset}} \quad \dots\text{eq (1)}$$

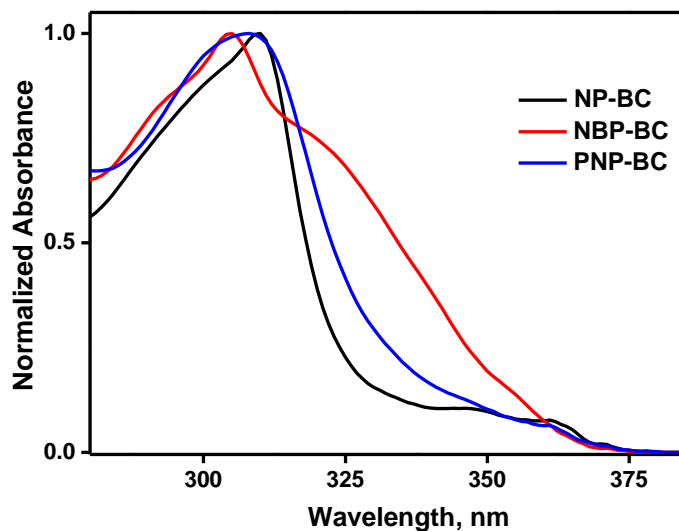


Figure S9. UV-vis absorption spectra of carbazole derivatives in solution (CH_2Cl_2).

The films were made by the spin-coating technique. The concentration of the compound used for spin-coating is ca. 4 mg/mL of dichloromethane. The spin-casted films were air-dried, and then UV-vis absorption spectrum was recorded. The UV-vis absorption spectrum of the bicarbazole derivatives were recorded in dichloromethane solution with a concentration of ca. 1.0×10^{-5} M.

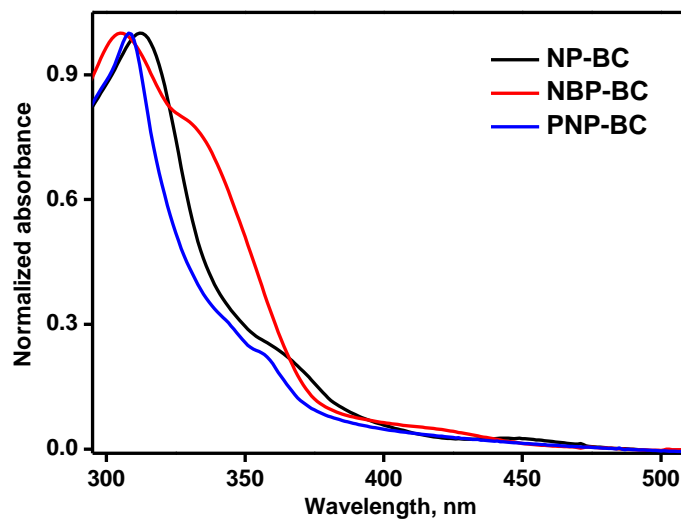


Figure S10. UV-vis absorption spectra of thin films of the carbazole derivatives.

Electrochemical properties of bicarbazole derivatives were evaluated by cyclic voltammetry (CV) measurements. The experiments were carried out as reported in the literature.²⁰ CV of all the compounds were recorded in dichloromethane solution containing 0.1 M TBAPF₆ as the supporting electrolyte. The concentration of the bicarbazole derivatives were maintained ca. 1.0 mM. After recording of the cyclic voltammograms of the pure bicarbazole derivatives, to this same solution, tiny amount of the ferrocene was introduced as the internal standard and the scans were run again.

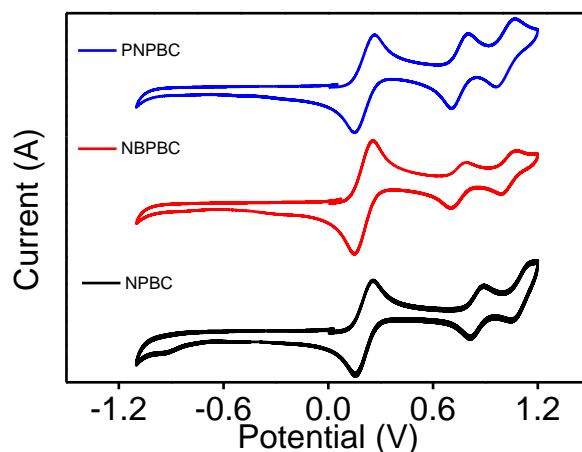


Figure S11. Cyclic voltammograms of the BCs, with Fc/Fc⁺ as internal standard, in CH₂Cl₂.

Extraction of HOMO values from the CV data

The HOMO values of the bicarbazole derivatives were derived from the onset oxidation potentials (in the cyclic voltammograms) of the compound and of the ferrocene using the following equation (1).¹ The values are summarized in Table S3. Formula for the HOMO value calculation from the CV data using the Fc/Fc⁺ as the internal standard is:¹

$$E_{\text{HOMO}} \text{ (eV)} = -(E_{\text{OX}}^{\text{onset}} - E_{\text{Fc/Fc}^+}^{\text{onset}}) - 4.80 \text{ eV} \quad \dots \text{eq (2)}$$

The energy values were calculated by using ferrocene as the internal standard with the HOMO value -4.8 eV against vacuum level as zero.^{1b} Here, $E_{\text{OX}}^{\text{onset}}$ and $E_{\text{Fc/Fc}^+}^{\text{onset}}$ are the onset oxidation potentials of the bicarbazole derivatives and of the ferrocene against Ag/AgCl electrode. The obtained ferrocene onset value was found to be in good agreement with the literature value.^{1e}

Table S3. Calculated HOMO energy levels for NP-BC, PNP-BC, and NBP-BC.

S. No.	Compound	E_{ox} (Onset, V)	Fc/Fc ⁺ , E_{ox} (Onset, V)	E_{HOMO} (eV)
1	NP-BC	0.7900	0.1400	-5.45
2	PNP-BC	0.7017	0.1324	-5.37
3	NBP-BC	0.6985	0.1324	-5.37

E_g value calculation from the UV-visible spectra

The LUMO values² were calculated by summing up the band gap (E_g , obtained from the onset of the UV-visible absorption spectrum) and the HOMO values (obtained from the oxidation onset of the cyclic voltammogram). The equation² is as follows and the values are tabulated in Table S4.

$$E_{\text{LUMO}} = E_{\text{HOMO}} + E_g \text{ (eV)} \quad \dots\text{eq (3)}$$

Table S4. Calculated LUMO energy levels for **NP-BC**, **PNP-BC**, and **NBP-BC**.

Compound	λ^{onset} (nm) soln/film	E_g (eV) soln/film	HOMO (eV)	LUMO (eV)
NP-BC	379/389	3.27/3.18	-5.45	-2.18/-2.27
PNP-BC	377/386	3.29/3.21	-5.37	-2.08/-2.16
NBP-BC	377/386	3.29/3.21	-5.37	-2.08/-2.16

5. Thermal properties (DSC)

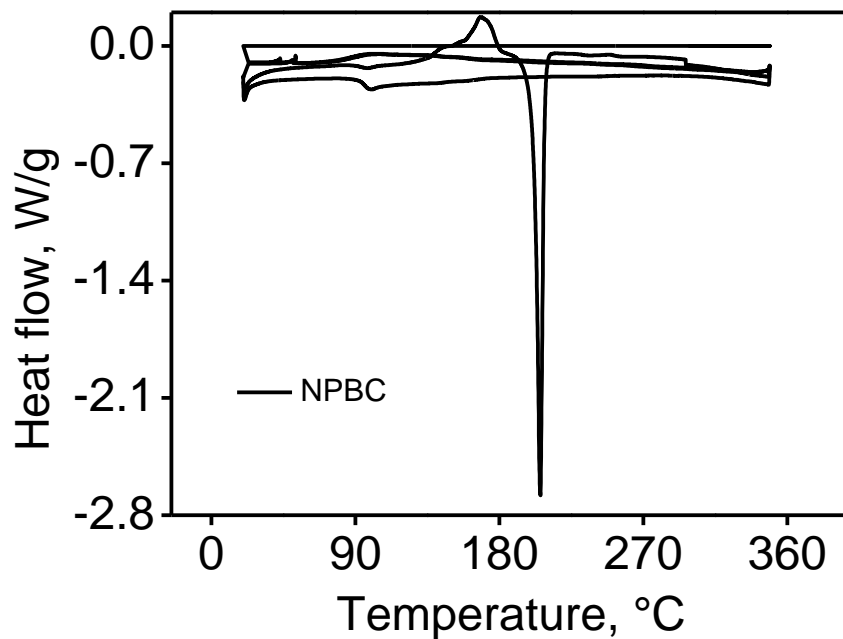


Figure S12. DSC trace of NP-BC under N₂ at a scanning rate of 10 °C min⁻¹.

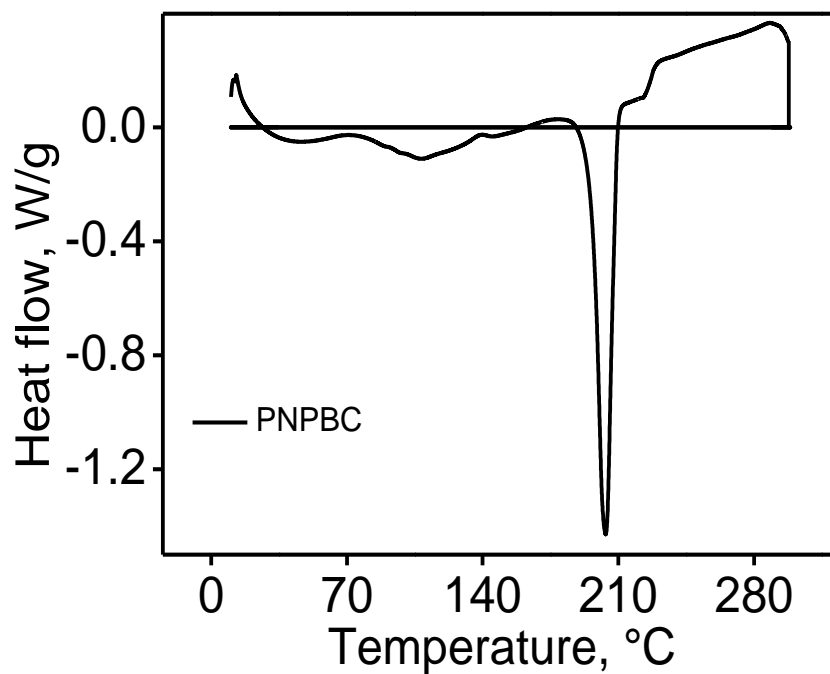


Figure S13. DSC trace of PNP-BC under N₂ at a scanning rate of 10 °C min⁻¹.

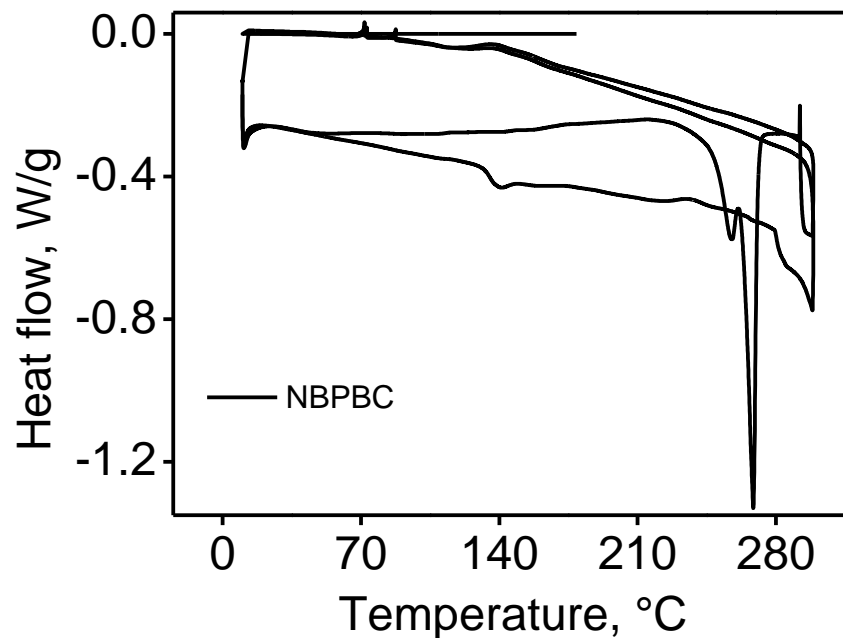


Figure S14. DSC trace of **NBP-BC** under N_2 at a scanning rate of $10\text{ }^\circ\text{C min}^{-1}$.

6. Theoretical calculation

Table S5. Calculated Low-Lying Transition for **BC-HTMs**

dye	state	excitation ^a	λ_{cal} (eV, nm)	f^b	Dipole moment (Debye)
NP-BC	S1	68.25% H→L	3.52(352)	0.5728	0.8595
	S2	68.43% H→L+1	3.58(346)	0.0171	
	S3	67.93% H→L+2	3.73(331)	0.0056	
NBP-BC	S1	67.915% H→L	3.74(330)	0.0060	0.7895
	S2	67.24% H→L+1	3.79(326)	0.0367	
	S3	68.25% H→L+2	3.95(313)	0.5618	
PNP-BC	S1	67.31% H→L	3.68(336)	0.0028	1.0377
	S2	66.08% H→L+1	3.72(332)	0.0083	
	S3	64.32% H→L+2	3.91(317)	0.6573	

^aH=HOMO, L=LUMO, L+2=LUMO+2, and L+1=LUMO+1. ^bOscillator strengths.

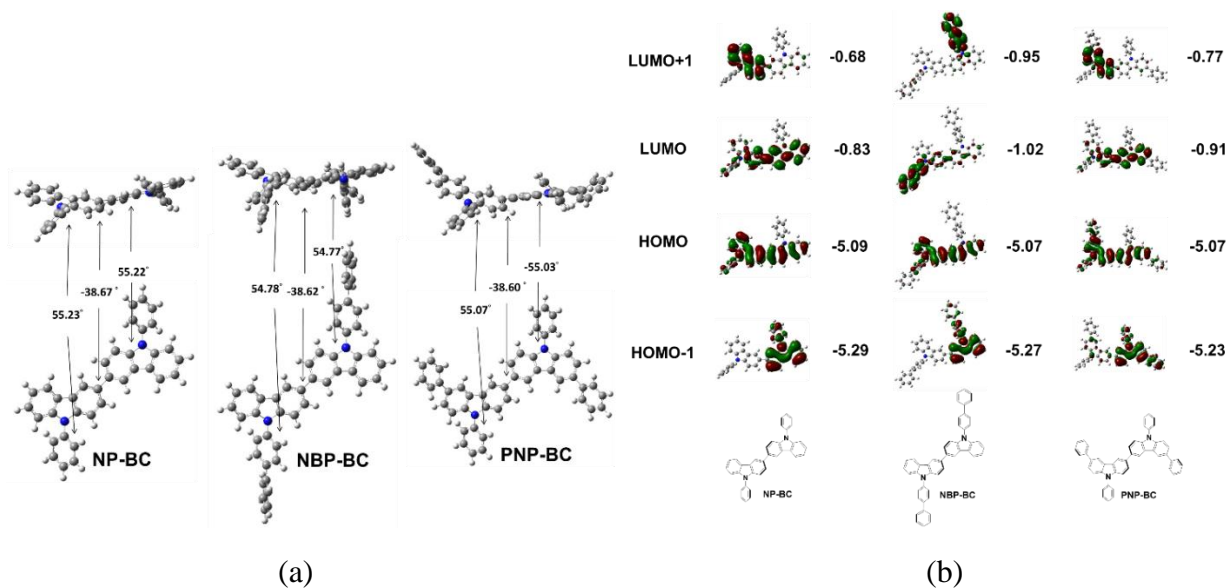


Figure S15. (a) Computed dihedral angles and (b) computed HOMO and LUMO energy levels and molecular orbitals of the **BC**-series HTMs.

7. UV, TRPL and PL spectra

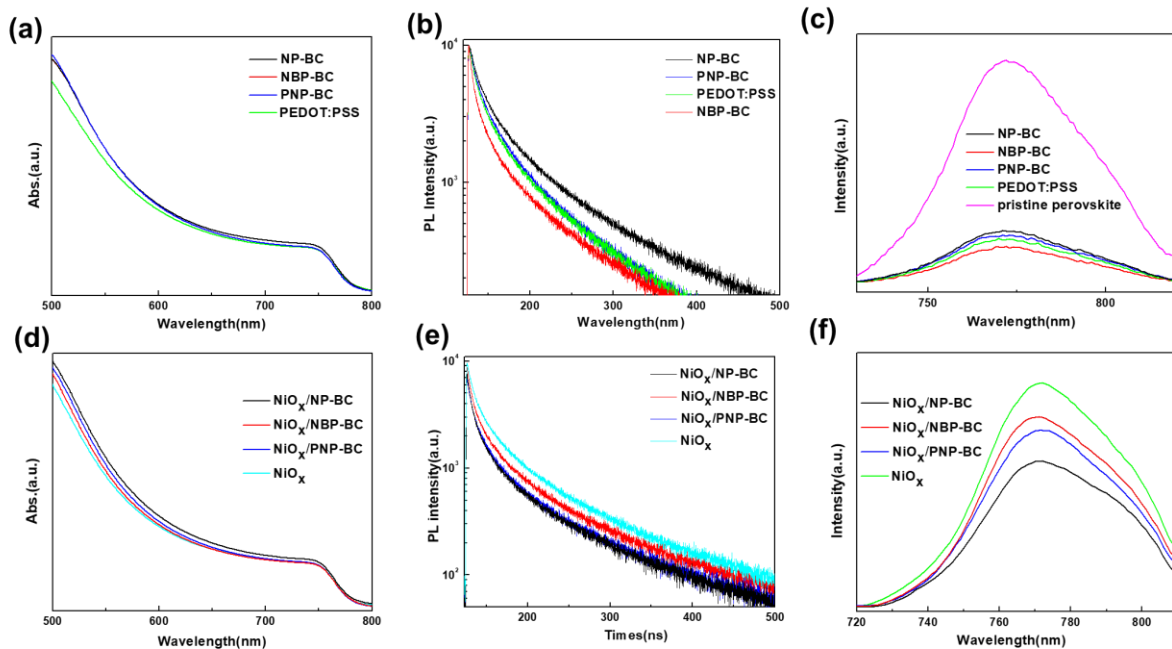


Figure S16. (a, d) UV-Vis, (b, e) TRPL, and (c, f) PL spectra of perovskite films spin-coated on the HTMs

8. Contact angle and surface energy

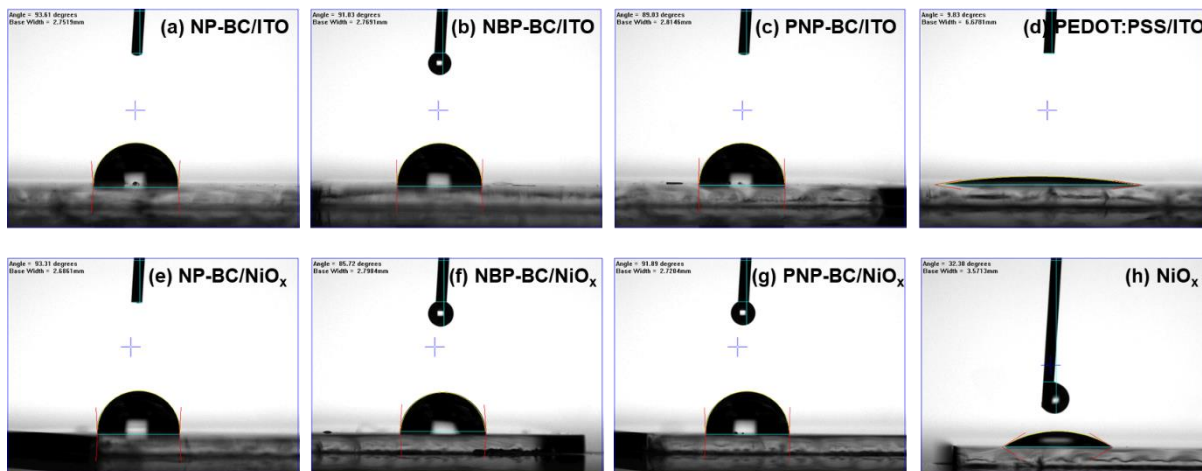


Figure S17. Water contact angles of BC-HTMs films on ITO and ITO/NiO_x substrates.

Table S6. Water contact angles, diiodomethane contact angles, and surface energies of the HTMs films.

HTM	$\theta_{\text{water}} (^{\circ})$	$\theta_{\text{Diiodomethane}} (^{\circ})$	$\gamma_{\text{total}} (\text{mN}\cdot\text{m}^{-1})$
NP-BC	93.61	16.24	50.88
NBP-BC	91.03	19.8	50.95
PNP-BC	89.03	15.38	52.68
PEDOT:PSS	9.83	28.24	82.08
NP-BC/NiO _x	93.31	16.07	51.02
NBP-BC/NiO _x	85.72	20.66	52.69
PNP-BC/NiO _x	91.89	17.49	51.20
NiO _x	32.30	23.69	76.27

^a The HTM was annealed at 100°C for 10 min.

9. XRD spectra

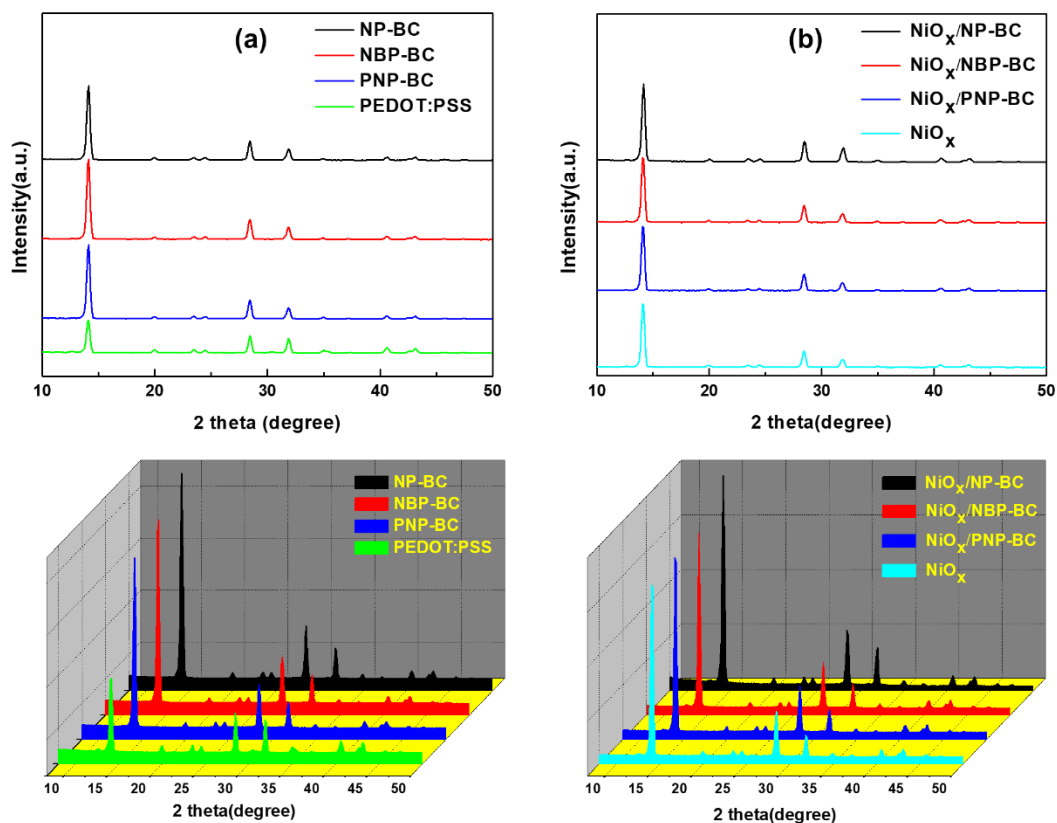


Figure S18. XRD spectra of perovskite films deposited on (a) NP-BC, NBP-BC, PNP-BC, and PEDOT:PSS as HTMs and (b) NiO_x/NP-BC, NiO_x/NBP-BC, NiO_x/PNP-BC, and bare NiO_x as HTMs.

10. PSC device stability

Table S7. Variation of the performance of PSCs in device types I and II.

HTM	J_{sc} (mA·cm ⁻²)	V_{oc} (V)	FF(%)	PCE (%)
NP-BC(0 hr)^a	16.61	0.986	65.0	10.637
NP-BC(168 hr)^a	18.10	0.964	61.0	10.645
NP-BC(336 hr)^a	16.34	0.970	65.5	10.384
NP-BC(504 hr)^a	17.60	0.957	60.6	10.209
NP-BC(672 hr)^a	17.44	0.960	61.0	10.219
NP-BC(804 hr)^a	18.14	0.960	60.8	10.637
NP-BC(1000 hr)^a	17.37	0.961	60.0	10.006
NBP-BC(0 hr)^a	20.84	0.977	64.0	13.037
NBP-BC(168 hr)^a	18.56	0.975	68.7	12.440
NBP-BC(336 hr)^a	18.04	0.972	69.6	12.210
NBP-BC(504 hr)^a	18.42	0.983	67.3	12.192
NBP-BC(672 hr)^a	18.33	0.961	68.6	12.093
NBP-BC(840 hr)^a	18.46	0.968	65.5	11.700
NBP-BC(1000 hr)^a	18.66	0.981	63.5	11.618
PNP-BC(0 hr)^a	22.14	0.949	58.5	12.277
PNP-BC(168 hr)^a	17.74	0.979	69.2	12.009
PNP-BC(336 hr)^a	17.99	0.977	66.0	11.605
PNP-BC(504 hr)^a	18.06	0.978	65.3	11.540
PNP-BC(672 hr)^a	18.81	0.971	61.6	11.248
PNP-BC(840 hr)^a	19.80	0.946	58.9	11.023
PNP-BC(1000 hr)^a	20.07	0.972	56.2	10.970
PEDOT:PSS(0 hr)^a	18.42	0.983	67.3	12.192
PEDOT:PSS(168 hr)^a	18.62	0.975	64.6	11.731
PEDOT:PSS(336 hr)^a	17.77	0.950	69.6	11.693
PEDOT:PSS(504 hr)^a	17.99	0.977	66.0	11.605
PEDOT:PSS(672 hr)^a	16.91	0.967	56.7	9.274
PEDOT:PSS(840 hr)^a	16.99	0.925	60.6	9.521
PEDOT:PSS(1000 hr)^a	17.82	0.904	50.3	8.103

NP-BC/NiO_x(0 hr)^b	22.37	1.071	79.5	19.064
NP-BC/NiO_x(168 hr)^b	22.34	1.059	76.9	18.196
NP-BC/NiO_x(336 hr)^b	22.04	1.045	77.8	17.918
NP-BC/NiO_x(504 hr)^b	22.32	1.035	77.4	17.878
NP-BC/NiO_x(672 hr)^b	22.11	1.047	76.3	17.666
NP-BC/NiO_x(840 hr)^b	22.45	1.034	74.9	17.378
NP-BC/NiO_x(1000 hr)^b	21.73	1.035	76.9	17.311
NBP-BC/NiO_x(0 hr)^b	21.64	1.086	76.5	17.984
NBP-BC/NiO_x(168 hr)^b	21.54	1.050	77.5	17.534
NBP-BC/NiO_x(336 hr)^b	21.11	1.046	79.2	17.486
NBP-BC/NiO_x(504 hr)^b	20.87	1.053	79.3	17.440
NBP-BC/NiO_x(672 hr)^b	21.28	1.049	77.3	17.260
NBP-BC/NiO_x(840 hr)^b	21.34	1.056	75.1	16.911
NBP-BC/NiO_x(1000 hr)^b	20.23	1.053	73.1	15.577
PNP-BC/NiO_x(0 hr)^b	22.18	1.057	80.4	18.850
PNP-BC/NiO_x(168 hr)^b	21.81	1.086	78.0	18.472
PNP-BC/NiO_x(336 hr)^b	21.74	1.067	76.1	17.649
PNP-BC/NiO_x(504 hr)^b	21.54	1.054	78.2	17.744
PNP-BC/NiO_x(672 hr)^b	21.43	1.064	77.9	17.749
PNP-BC/NiO_x(840 hr)^b	21.46	1.049	78.4	17.646
PNP-BC/NiO_x(1000 hr)^b	20.45	1.040	76.7	16.299
NiO_x(0 hr)^b	20.11	1.043	75.5	15.836
NiO_x(168 hr)^b	19.95	1.054	74.5	15.663
NiO_x(336 hr)^b	20.00	1.052	74.2	15.606
NiO_x(504 hr)^b	19.80	1.019	72.7	14.662
NiO_x(672 hr)^b	19.62	1.016	73.2	14.585
NiO_x(840 hr)^b	20.37	1.016	69.6	14.405
NiO_x(1000 hr)^b	19.43	1.023	72.1	14.337

^a Device type I: ITO/HTM/perovskite/PC₆₁BM/BCP/Ag. ^b Device type II: ITO/NiO_x/interfacial layer /perovskite/PC₆₁BM/BCP/Ag.

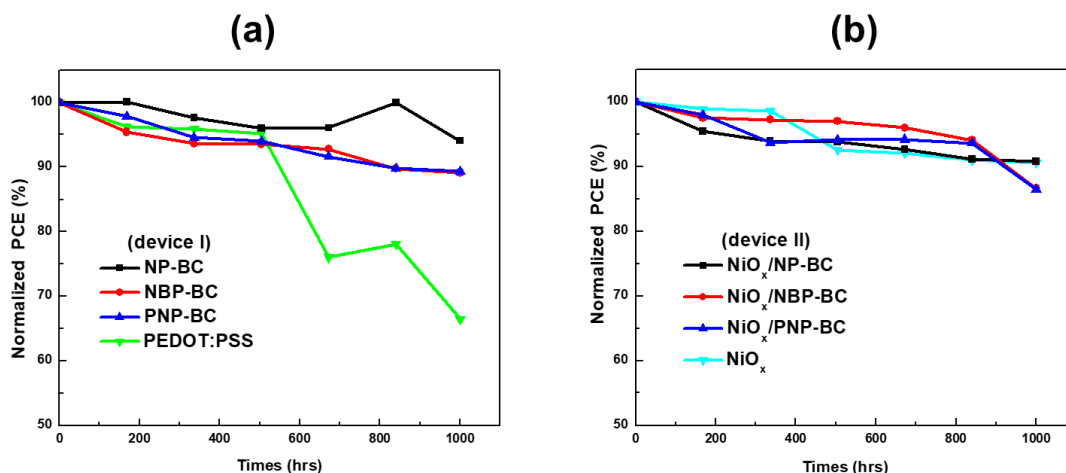


Figure S19. Stability tests of the PSCs incorporating (a) NP-BC, NBP-BC, PNP-BC, and PEDOT:PSS as HTMs (device I) and (b) NiO_x/NP-BC, NiO_x/NBP-BC, NiO_x/PNP-BC, and bare NiO_x as HTMs (device II).

References

- 1) a) Kumada, M.; Tamao, K. Aliphatic Organopolysilanes. *Adv. Organomet. Chem.* **1968**, *6*, 19-117. b) Pommerehne, J.; Vestweber, H.; Guss, W.; Mahrt, R. F.; Bässler, H.; Porsch, M.; Daub, J. Efficient Two Layer Leds on a Polymer Blend Basis. *Adv. Mater.* **1995**, *7*, 551-554. c) D'Andrade, B. W.; Datta, S.; Forrest, S. R.; Djurovich, P.; Polikarpov, E.; Thompson, M. E. Relationship Between the Ionization and Oxidation Potentials of Molecular Organic Semiconductors. *Org. Electron.* **2005**, *6*, 11-20. d) Liu, Y.; Liu, M. S.; Jen, A.K.-Y. Synthesis and Characterization of a Novel and Highly Efficient Light-Emitting Polymer. *Acta Polym.* **1999**, *50*, 105-108. e) Tsierkezos, N. G. Cyclic Voltammetric Studies of Ferrocene in Non-aqueous Solvents in the Temperature Range from 248.15 to 298.15 K. *J. Solution. Chem.* **2007**, *36*, 289-302.
- 2) Seguy, I.; Jolinat, P.; Destruel, P.; Farenc, J. Red Organic Light Emitting Device Made from Triphenylene Hexaester and Perylene Tetraester. *J. Appl. Phys.* **2001**, *89*, 5442-5448.
- 3) Zhou, Y.; Verkade, J. G. Highly Efficient Ligands for the Palladium-Assisted Double N-Arylation of Primary Amines for One-step Construction of Carbazoles. *Adv. Synth. Catal.* **2010**, *352*, 616-620.

- 4) Steihoff, G. W.; Henry, M. C. Reaction of Benzyne with Nitrosobenzene. A New Route to the Carbazole Ring System, *J. Org. Chem.* **1964**, *9*, 2808-2809.
- 5) Chen, F.; Liu, N.; Ji, E.; Dai, B. Copper/ β -Diketone-Catalyzed-*N*-Arylation of Carbazoles. *RSC Adv.* **2015**, *5*, 51512-51523.
- 6) Yoo, W.-J.; Tsukamoto, T.; Kobayashi, S. Visible Light-Mediated Ullmann-Type C-N Coupling Reactions of Carbazole Derivatives and Aryl Iodides. *Org. Lett.* **2015**, *17*, 3640-3642.
- 7) Wei, B. B.; Liu, J.-Z.; Zhang, Y.; Zhang, J.-H.; Peng, H.-N.; Fan, H.-L.; He, Y.-B.; Gao, X.-C. Stable, Glassy, and Versatile Binaphthalene Derivatives Capable of Efficient Hole Transport, Hosting, and Deep-Blue Light Emission. *Adv. Funct. Mater.* **2010**, *20*, 2448-2458..
- 8) Wang, L.; Ji, E.; Liu, N.; Dai, B. Site-Selective *N*-Arylation of Carbazoles with Halogenated Fluorobenzenes. *Synthesis* **2016**, *48*, 737-750.
- 9) Tao, S.; Liu, N.; Dai, B. One-Pot Two-Step Synthesis of *N*-Arylcarbazole Based Skeleton. *RSC Adv.* **2016**, *6*, 43250-43260.
- 10) Yu, F.-F.; Fan, H.-L.; Huang, H.-F.; Cao, Q.-Y.; Dai, Y.-F.; Gao, X.-C.; Shang, Y.-Z.; Zhang, M.-Y.; Long, L.; Xu, H.; Li, X.-F.; Wei, B. Blue Fluorescence from the Ligand and Yellow Phosphorescence from the Iridium Complex: High-Efficiency Wet-Processed White Organic Light-Emitting Device. *Inorganica Chimica Acta.* **2012**, *390*, 119-122.
- 11) Kim, Y. E.; Kwon, Y. S.; Lee, K. S.; Park, J. W.; Seo, H. J.; Kim, T. W. Synthesis and Electrochemical Properties of *N*-Substituted Bicarbazyl Derivatives. *Mol. Cryst. Liq. Cryst.* **2004**, *424*, 153-158.
- 12) Kim, J. K.; Kim, Y.-K.; Min, S.-H.; Yu, E. S.; Kim, B.-K.; Lee, B.-K.; Jang, K.; Jung, S.-H. Preparation of Carbazole Derivatives for Organic Optoelectronic Device. *PCT Int. Appl.* WO 2017034085 A1, Mar 02, 2017
- 13) Ji, H. S.; Moon, S. Y.; Park, J. C.; Park, Y. U.; Kang, M. S.; Lee, B.S.; Kim, S. H. Organic Electronic Element Containing Light EfficiencyImproving Layer and Electronic Device Containing the Same. *Repub. Korean Kongkae Taeho Kongbo* KR 2015012835 A, 2015.

- 14) Maciejczyk, M.; Ivaturi, A.; Robertson, N. SFX as a Low-Cost ‘Spiro’ Hole-Transport Material for Efficient Perovskite Solar Cells. *J. Mater. Chem. A* **2016**, *4*, 4855-4863.
- 15) Saliba, M.; Orlandi, S.; Matsui, T.; Aghazada, S.; Cavazzini, M.; Correa-Baena, J.-P.; Gao, P.; Scopelliti, R.; Mosconi, E.; Dahmen, K.-H.; Angelis, F. D.; Abate, A.; Hagfeldt, A.; Pozzi, G.; Grätzel, M.; Nazeeruddin, M. K. A Molecularly Engineered Hole-Transporting Material for Efficient Perovskite Solar Cells. *Nature Energy* **2016**, *1*, 15017.
- 16) Xu, B.; Bi, D.; Hua, Y.; Liu, P.; Cheng, M.; Grätzel, M.; Kloo, L.; Hagfeldt, A.; Sun, L. A Low-Cost Spiro[fluorene-9,9'-xanthene]-Based Hole Transport Material for Highly Efficient Solid-State Dye-Sensitized Solar Cells and Perovskite Solar Cells. *Energy Environ. Sci.* **2016**, *9*, 873-877.
- 17) Chen, Y.-C.; Huang, S.-K.; Li, S.-S.; Tsai, Y.-Y.; Chen, C.-P.; Chen, C.-W.; Chang, Y. J. Facilely Synthesized spiro[fluorene-9,9'-phenanthren-10'-one] in Donor–Acceptor–Donor Hole-Transporting Materials for Perovskite Solar Cells. *ChemSusChem* **2018**, *11*, 3225-3233.
- 18) Pham H. D.; Do, T. T.; Kim, J.; Charbonneau, C.; Manzhos, S.; Feron, K.; Tsoi, W. C.; Durrant, J. R.; Jain, S. M.; Sonar, P. Molecular Engineering Using an Anthanthrone Dye for Low-Cost Hole Transport Materials: A Strategy for Dopant-Free, High-Efficiency, and Stable Perovskite Solar Cells. *Adv. Energy Mater.* **2018**, 1703007.
- 19) Petrus, M. L.; Schutt, K.; Sirtl, M. T.; Hutter, E. M.; Closs, A. C.; Ball, J. M.; Bijleveld, J. C.; Petrozza, A.; Bein, T.; Dingemans, T. J. New Generation Hole Transporting Materials for Perovskite Solar Cells: Amide-Based Small-Molecules with Nonconjugated Backbones. *Adv. Energy Mater.* **2018**, *8*, 1801605
- 20) Yeh, S. J.; Tsai, C. Y.; Huang, C.-Y.; Liou, G.-S.; Cheng, S.-H. Electrochemical Characterization of Small Organic Hole-Transport Molecules Based on the Triphenylene Unit. *Electrochem. Commun.* **2003**, *5*, 373-377.